



**NIST Special Publication 260**  
**NIST SP 260-263**  
**Certification of Standard Reference**  
**Material<sup>®</sup> 2921a**

*Human Cardiac Troponin Complex*

David M. Bunk  
David Newton

This publication is available free of charge from:  
<https://doi.org/10.6028/NIST.SP.260-263>

**NIST Special Publication 260**  
**NIST SP 260-263**

# **Certification of Standard Reference Material<sup>®</sup> 2921a**

*Human Cardiac Troponin Complex*

David M. Bunk  
*Biomolecular Measurement Division  
National Institute of Standards and  
Technology*

David Newton  
Statistical Engineering Division  
National Institute of Standards and Technology

This publication is available free of charge from:  
<https://doi.org/10.6028/NIST.SP.260-263>

January 2026



U.S. Department of Commerce  
*Howard Lutnick, Secretary*

National Institute of Standards and Technology  
*Craig Burkhardt, Acting Under Secretary of Commerce for Standards and Technology and Acting NIST Director*

Certain equipment, instruments, software, or materials, commercial or non-commercial, are identified in this paper to specify the experimental procedure adequately. Such identification does not imply recommendation or endorsement of any product or service by NIST, nor does it imply that the materials or equipment identified are necessarily the best available for the purpose.

#### **NIST Technical Series Policies**

[Copyright, Use, and Licensing Statements](#)

[NIST Technical Series Publication Identifier Syntax](#)

#### **Publication History**

Approved by the NIST Editorial Review Board on 2025-12-19

#### **How to Cite this NIST Technical Series Publication**

Bunk DM, Newton D (2026) Certification of Standard Reference Materials 2921a. (National Institute of Standards and Technology, Gaithersburg, MD), NIST Special Publication (NIST SP) 260-263.

<https://doi.org/10.6028/NIST.SP.260-263>

#### **Author ORCID iDs**

David M. Bunk: 0009-0007-2187-4224

David Newton: 0000-0003-3382-8034

#### **Technical Information Contact for this SRM**

Please address technical questions about this SRM to [srms@nist.gov](mailto:srms@nist.gov), where they will be assigned to the appropriate Technical Project Leader responsible for supporting this material. For sales and customer service inquiries, please contact [srminfo@nist.gov](mailto:srminfo@nist.gov).

## **Abstract**

The National Institute of Standards and Technology (NIST) Standard Reference Material® (SRM®) 2921a Human Cardiac Troponin Complex delivers a certified value for the concentration of human cardiac troponin I in a solution of the human cardiac troponin complex and the associated uncertainty of the certified value. The material is intended for 1) use in validating measurement procedures and 2) use in qualifying control materials produced in-house and analyzed using measurement methods for the determination of the concentration of human cardiac troponin I in human blood samples. A unit of SRM 2921a consists of three (3) vials of a frozen aqueous solution of human cardiac troponin complex. This publication documents the production, measurement processes, results, and statistical evaluations involved in the production and certification of SRM 2921a.

## **Keywords**

Human Cardiac Troponin Complex, Cardiac Troponin I (cTnI), Cardiac Troponin T (cTnT), Cardiac Troponin C (cTnC), Standard Reference Material (SRM).

## Table of Contents

<b>1. Author Contributions</b> .....	<b>v</b>
<b>2. INTRODUCTION</b> .....	<b>1</b>
<b>3. PRODUCTION OF SRM 2921a</b> .....	<b>2</b>
3.1. ACQUISITION OF PURIFIED HUMAN CARDIAC TROPONIN COMPLEX.....	2
3.2. PRODUCTION OF THE BULK SRM 2921a SOLUTION AND ALIQUOTTING .....	2
<b>4. Qualitative Assessment of the Troponin Complex Subunits in SRM 2921a</b> .....	<b>4</b>
<b>5. SRM 2921A Certification Plan and Method Development</b> .....	<b>16</b>
5.1. Evaluating Mobile Phase Additives .....	18
5.2. SIM Method Development.....	19
5.3. Optimization of Chromatographic Column Clean-up .....	22
<b>6. Certification Measurements of SRM 2921a by LC-MS using Selected Ion Monitoring</b> .....	<b>24</b>
6.1. Certification Measurement Results for SRM 2921a.....	26
<b>7. Statistical Evaluation of SRM 2921a Certification Data</b> .....	<b>27</b>
7.1. Statistical Modeling.....	28
<b>8. Certification Measurement Results</b> .....	<b>30</b>
<b>9. SRM 2921a Measurement Claim</b> .....	<b>33</b>
<b>10. Measurement Traceability</b> .....	<b>34</b>
<b>11. Homogeneity Assessment</b> .....	<b>35</b>
<b>12. References</b> .....	Error! Bookmark not defined.
<b>Appendix A. Fitzgerald Industries Certificate of Analysis</b> .....	<b>39</b>
<b>Appendix B. Experimental details of the Qualitative LC-MS analysis of SRM 2921a</b> .....	<b>40</b>
<b>Appendix C. Agilent LC-MS SIM Method Parameters</b> .....	<b>42</b>
<b>Appendix D. Agilent LC-MS Needle and Column Wash Method Parameters</b> .....	<b>45</b>
<b>Appendix E. Typical worklist for the acquisition of certification data from a measurement set</b> .....	<b>47</b>
<b>Appendix F. Certification data from the LC-MS analysis of SRM 2921a using SIMS.</b> .....	<b>50</b>
<b>Appendix G. Gravimetric sample and calibration solutions preparation data and raw analysis data from certification sets</b> .....	<b>52</b>
<b>Appendix H. Additional statistical results from hierarchical calibration model</b> .....	<b>62</b>

## List of Tables

<b>Table 1.</b> Calculated and observed masses for the identified peaks in the deconvoluted mass spectra of cTnT for SRM 2921a.....	<b>7</b>
<b>Table 2.</b> Calculated and observed masses for the identified peaks in the deconvoluted mass spectra of cTnI for SRM 2921a.....	<b>10</b>

<b>Table 3.</b> Calculated and observed masses for the identified peak in the deconvoluted mass spectra of cTnC for SRM 2921a.....	<b>13</b>
<b>Table 4.</b> Comparison of LC-MS peak areas for replication injections of samples prepared from SRM 2921A using 0.5 % formic acid and 0.1 % TFA as mobile phase additive.....	<b>19</b>
<b>Table 5.</b> Evaluation of the dilution buffer used to prepare samples and calibrators for the certification of SRM 2921a by LC-MS. Note that averages and standard deviations were calculated using the last 5 LC-MS runs in each set of 6 replicate injections.....	<b>21</b>
<b>Table 6.</b> Comparison of sample worklists for the evaluation of needle and column washes on peak area reproducibility.....	<b>22</b>
<b>Table 7.</b> Comparison of the peak area reproducibility of replicate injections of a calibrator prepared from SRM 2921 with and without injector needle washes between injections.....	<b>23</b>
<b>Table 8.</b> Calibration curve parameters from the five sets of calibration data. ....	<b>25</b>
<b>Table 9.</b> Averaged measurement results for the cTnI concentration in SRM 2921a. The standard deviations listed are from the measured concentration values and do not reflect the expanded uncertainty .....	<b>26</b>
<b>Table 10.</b> Model results.....	<b>32</b>
<b>Table 11.</b> Measurement claim for cTnI concentration in SRM 2921a.....	<b>33</b>
<b>Table 12.</b> ANOVA model results for fitting set and box as a function of cTnI. ....	<b>36</b>

### List of Figures

<b>Figure 1.</b> Total Ion Chromatogram (TIC) from the LC-MS analysis of A) SRM2921a and B) SRM 2921.....	<b>4</b>
<b>Figure 2.</b> Averaged mass spectra from the peak associated with cTnT in A) SRM 2921a, and B) SRM 2921 .....	<b>5</b>
<b>Figure 3.</b> Deconvoluted mass distributions of the cTnT peak for A) SRM 2921a and B) SRM 2921. Tentative identifications of cTnT proteoforms of the major masses are assigned to peaks in A). Spectral deconvolution was performed using Agilent MassHunter BioConfirm software. ....	<b>6</b>
<b>Figure 4.</b> Averaged mass spectra from the peak associated with cTnI in A) SRM 2921a, and B) SRM 2921	<b>8</b>
<b>Figure 5.</b> Deconvoluted mass distributions of the cTnI peak for A) SRM 2921a and B) SRM 2921. Tentative identifications of cTnI proteoforms of the major masses are assigned to peaks in A). Spectral deconvolution was performed using Agilent MassHunter BioConfirm software. ....	<b>9</b>
<b>Figure 6.</b> Averaged mass spectra from the peak associated with cTnC in A) SRM 2921a, and B) SRM 2921. ....	<b>12</b>
<b>Figure 7.</b> Deconvoluted mass distributions of the cTnC peak for A) SRM 2921a and B) SRM 2921. Tentative identification of the cTnC proteoform is assigned to the peak with the highest signal abundance in A). Spectral deconvolution was performed using Agilent MassHunter BioConfirm software. ....	<b>13</b>
<b>Figure 8.</b> Deconvoluted mass distributions of the peak designated as “Impurity 1” in Figure 1 for A) SRM 2921a, and B) SRM 2921. ....	<b>14</b>
<b>Figure 9.</b> Averaged mass spectra from the peak designated as “Impurity 2” in Figure 1 for A) SRM 2921a, and B) SRM 2921. ....	<b>15</b>

<b>Figure 10.</b> Total ion chromatogram (TIC) from the LC-MS analysis of A) purified cTnI, and B) SRM 2921a .....	<b>16</b>
<b>Figure 11.</b> Averaged spectra from the peak associated with cTnI in A) the purified cTnI material, and B) SRM 2921a.....	<b>17</b>
<b>Figure 12.</b> Comparison of the chromatographic separation of dilutions of SRM 2921a using A) 0.5 % (v/v) formic acid and B) 0.1 % (v/v) trifluoroacetic acid as mobile phase additive. ....	<b>18</b>
<b>Figure 13.</b> Averaged mass spectra from the cTnI chromatographic peak in the LC-MS analysis of A) SRM 2921a and B) SRM 2921. ....	<b>19</b>
<b>Figure 14.</b> Dilution scheme for the quantification of cTnI concentration in SRM 2921a using calibrators prepared from SRM 2921. ....	<b>20</b>
<b>Figure 15.</b> Total ion chromatogram from the LC-MS analysis in SIM mode of A) calibration sample prepared from SRM 2921, and B) sample prepared from SRM 2921a.....	<b>24</b>
<b>Figure 16.</b> Calibration curve from the bracketing calibration for certification set 1.....	<b>25</b>
<b>Figure 17.</b> Data used for calibration functions. Points represent LC-MS data (peak areas) from calibrants prepared from SRM 2921, and diagonal lines represent estimated calibration functions.....	<b>27</b>
<b>Figure 18.</b> Posteriors for individual SRM 2921a samples. Thin lines represent 95 % posterior intervals, thick blue lines represent 80 % posterior intervals, and points indicate the median of each posterior distribution. The solid vertical line represents the overall mean estimate, while dashed and dotted lines represent +/- one standard uncertainty and one expanded uncertainty, respectively. ....	<b>31</b>
<b>Figure 19.</b> The measured concentration of cTnI in SRM 2921a versus the box number from which the sample was chosen.....	<b>35</b>
<b>Figure 20.</b> The measured concentration of cTnI in SRM 2921a versus the box number from which the sample was chosen, separated by measurement set.....	<b>36</b>

## 1. Author Contributions

**David Bunk:** Conceptualization, Data curation, Formal analysis, Investigation, Methodology, Project administration, Software, Validation, Visualization, Writing-original draft.

**David Newton:** Formal analysis, Visualization, Writing- original draft.

## 2. INTRODUCTION

SRM 2921a Human Cardiac Troponin Complex is a buffered solution of the cardiac troponin complex extracted from human cardiac tissue. It is intended to be used as a quality assessment tool for clinical diagnostic laboratories and manufacturers of *in vitro* diagnostic tests that measure human cardiac troponin I. SRM 2921a is the replacement of SRM 2921 and is intended to be comparable in composition and the approximate concentration of human cardiac troponin I to that of SRM 2921.

The human cardiac troponin complex is composed of three protein subunits: cardiac troponin T (cTnT), cardiac troponin I (cTnI), and cardiac troponin C (cTnC). The stoichiometry of the complex in cardiac tissue is equimolar for each subunit (i.e., 1:1:1). The function of the human cardiac troponin complex in cardiac tissue is the regulation of cardiac muscle contraction [1]. The measurement of cTnT and cTnI in human blood samples (whole blood, serum, or plasma) has clinical diagnostic utility. The American Heart Association and the American College of Cardiology recommend the clinical measurement of either the cardiac troponin T (cTnT) or cardiac troponin I (cTnI) as “the preferred biomarker for diagnosing acute myocardial infarction” [2]. The amino acid sequences of both the human troponin T and the human troponin I found in cardiac tissue, are different than the skeletal muscle forms of these two proteins. The amino acid sequence of human cTnC is the same as the form found in skeletal muscle. As such, the measurement of the cardiac forms of the troponin T and troponin I subunits in blood samples is indicative of their release into the bloodstream following cardiac tissue damage. Chronically elevated troponin levels have also been associated with conditions such as congestive heart failure [3].

The measurement of cTnT for clinical diagnostic purposes was patented by Abbott Laboratories in 2009 [3]. Because of the patent (which expires in 2030), Abbott Laboratories licenses this measurement to other diagnostic assay manufacturers and supplies the antibodies used in all commercial immunoassays for cTnT. As a result, the clinical measurement of cTnT is less prevalent than that of cTnI. There is much better agreement among cTnT assays because they all use the same antibodies. The clinical measurement of cTnI is not patented. There are many commercial clinical assays for human cTnI, used in the diagnosis of myocardial infarction or the assessment of damage to heart tissue [4] and the antibodies used in the clinical cTnI assays are not all the same as those used for cTnT measurement. Assay standardization is needed [5] to bring measurement result comparability to the diverse set of commercial cTnI assays used for clinical diagnostics.

This report details the preparation and certification of the concentration of human cardiac troponin I in SRM 2921a using a liquid chromatography-mass spectrometry (LC-MS) analysis method calibrated with NIST SRM 2921. These measurements are intended for use in the final value assignment of the human cardiac troponin I concentration in SRM 2921a. Also included in this report are results from the qualitative assessment of the troponin T, troponin I, and troponin C subunits in SRM 2921a with comparison to the covalent protein structures of the corresponding subunits in SRM 2921.

### **3. PRODUCTION OF SRM 2921a**

Ideally, the human troponin complex protein in SRM 2921a should be similar to that in SRM 2921 in protein structure, as both materials are or will be used to support immunoassay measurements that are sensitive to changes in protein structure. The human troponin complex material used to prepare SRM 2921 was obtained from HyTest LTD (Turku, Finland). However, changes in the federal procurement rules prevented NIST from purchasing the material for SRM 2921a from this vendor. Prior to procuring the material needed to prepare SRM 2921a, small quantities of purified human troponin complex were obtained from vendors and compared to SRM 2921 using analytical techniques such as LC-MS/MS to evaluate protein structure.

An open solicitation for quotations was issued for the acquisition of the purified human cardiac troponin complex used for the preparation of SRM 2921a. The following Sections summarize the scope for the material acquisition, the production of the bulk SRM 2921a solution, and the aliquoting of the material.

#### **3.1. ACQUISITION OF PURIFIED HUMAN CARDIAC TROPONIN COMPLEX**

The contract for the acquisition of the material to produce SRM 2921a was awarded to Fitzgerald Industries International. Approximately 60 mg of purified human cardiac troponin complex (Fitzgerald Industries catalog number 30R-AT033) was purchased through contract number SB1341-16-SU-0758. The Fitzgerald Certificate of Analysis for this material is shown in Appendix A.

#### **3.2. PRODUCTION OF THE BULK SRM 2921a SOLUTION AND ALIQUOTTING**

The aqueous buffer for the preparation of the bulk solution of human cardiac troponin complex was composed of 20 mmol/L tris(hydroxymethyl)aminomethane (commonly referred to as “tris”), 150 mmol/L sodium chloride, and 5 mmol/L calcium chloride with a pH of approximately 7.6. The buffer was prepared by weighing the appropriate amounts of tris(hydroxymethyl)aminomethane, sodium chloride, and calcium chloride dihydrate and dissolving in 18 MΩ-cm water prepared from a Thermo Barnstead GenPure water polisher. The pH of the buffer solution was measured using a Mettler Toledo FiveEasy F20 pH meter, which had been calibrated with commercial pH 7.0 and pH 10.0 calibration solutions.

The bulk solution for SRM 2921a was prepared by diluting a concentrated solution of purified human cardiac troponin complex obtained from Fitzgerald Industries International with the aqueous buffer described above. Approximately 60 mg (52.6 mL of a 1.14 mg/mL solution, per the manufacturer’s certificate of analysis (Appendix A)) of purified human cardiac troponin complex was removed from a -80 °C freezer where it had been stored since acquisition from Fitzgerald. The frozen human cardiac troponin complex was thawed in a lukewarm water bath for approximately 2 h before being added to a tared clean 500 mL Teflon bottle on a Mettler

Toledo model MS3002TS balance. The measured weight of the Fitzgerald troponin complex solution added to the 500 mL Teflon bottle was approximately 50.52 g at room temperature (approximately 20 °C). The bottle containing the Fitzgerald troponin complex was repeatedly (5 times) rinsed with the buffer, and each rinse was added to the Teflon bottle containing the troponin complex. The total measured weight of buffer rinses was 361.61 g. A clean magnetic spin bar was added to the diluted troponin complex solution, and the solution was left stirring in a 5 °C refrigerator overnight on a magnetic stirring platform before aliquoting.

Based on the molecular masses of the troponin subunits and the manufacturer's reported concentration, the approximate mass of cardiac troponin I in the 60 mg of Fitzgerald human cardiac troponin complex is 18.3 mg. After dilution with approximately 361.61 mL of buffer (assuming the density of the buffer was approximately 1 g/mL at 25 °C), the expected concentration of the bulk solution of SRM 2921a is approximately 0.051 g/L. For comparison, the certified concentration of cardiac troponin I in SRM 2921 is 0.0312 g/L  $\pm$  0.0014 g/L (31.2 mg/L  $\pm$  1.4 mg/L).

Starting approximately one day after the initial preparation of the bulk solution of SRM 2921a and overnight stirring at 5 °C, aliquoting of SRM 2921a into vials took place over two consecutive days. The bulk solution, which had not yet been aliquoted, was stored at 5 °C between aliquoting sessions. An Eppendorf Research Pro 50-1000  $\mu$ L pipettor was used to manually pipette approximately 115  $\mu$ L aliquots using the repeat dispense pipette setting (8 x 115  $\mu$ L aliquots could be dispensed before resetting the pipettor). The aliquots of SRM 2921a were dispensed in labeled Sarstedt sterile 0.5 mL polypropylene screw-capped vials (part number 72.730.005). SRM 2921a was aliquoted in sets of 100 vials, which were immediately stored at -80 °C once each box was filled. Boxes 1 through 15 were filled on the first day of aliquoting; boxes 16 through 28 and a box of 80 vials were filled on the second day of aliquoting. The total number of vials filled was 2880 across 29 boxes.

#### 4. Qualitative Assessment of the Troponin Complex Subunits in SRM 2921a

To measure the molecular mass of the protein constituents in SRM 2921a, reversed-phase LC-MS was performed, acquiring high-resolution full-scan MS data using the Agilent model 6550A hybrid quadrupole-time of flight (QToF) mass spectrometer. Experimental details of the LC-MS analysis are listed in Appendix B. Replicate LC-MS qualitative analysis was performed on 4 vials each of SRM 2921a and SRM 2921. The total ion chromatogram (TIC) from one of the qualitative analyses of SRM 2921a is shown in Figure 1A. In Figure 1A, the main chromatographic peaks have been identified through their MS scans. As was observed in the original analysis of SRM 2921, the cTnT elutes first, followed by cTnI and then cTnC. Two other minor peaks, labeled "Impurity 1" and "Impurity 2" in Figure 1A, were also observed in every LC-MS analysis of SRM 2921a.

For comparison, Figure 1B shows the LC-MS TIC for the analysis of an undiluted aliquot of SRM 2921. The TICs for SRM 2921 are very similar to those of SRM 2921a, although the ratio of the peak intensities appear to be slightly different.

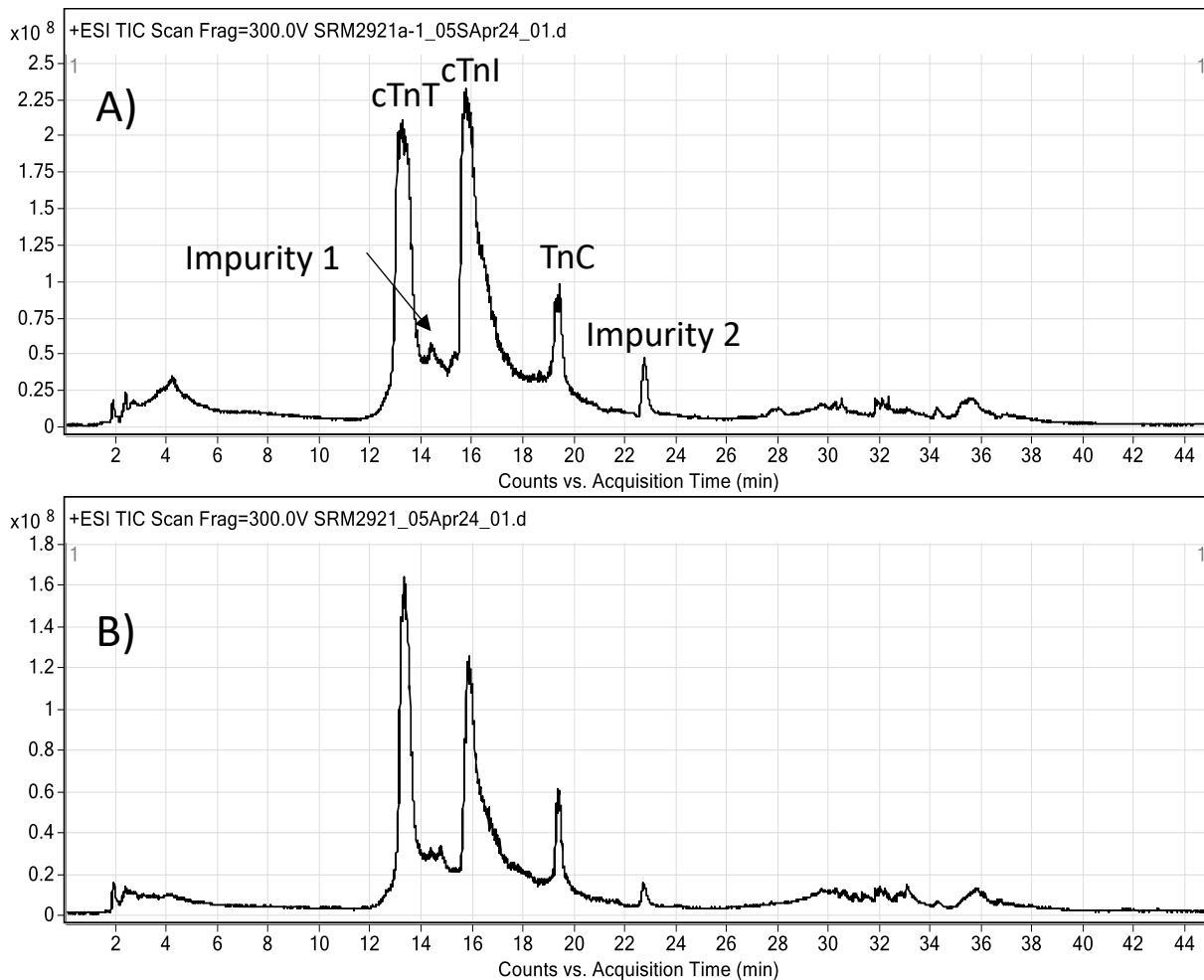


**Figure 1.** Total Ion Chromatogram (TIC) from the LC-MS analysis of A) SRM2921a and B) SRM 2921

Figure 2A shows the average of MS scans across the first chromatographic peak, centered at approximately 13.5 min in Figure 1A, for SRM 2921a. The averaged spectra in Figure 2A show a distribution of multiply-charged molecular ion peaks typical of a protein, based on the uneven spacing between peaks. The averaged spectrum from the same peak for an SRM 2921 sample is shown in Figure 2B. The charge state peak masses for both SRM 2921a and SRM 2921 are nearly identical. Deconvolution of the charge-state molecular ion peak distributions in Figures 2A and 2B is shown in Figures 3A and 3B, respectively. The calculated average molecular mass of the intact cTnT subunit is approximately 35791.9 Da. The cTnT average molecular mass was calculated from the amino acid sequence of cTnT [6] using the NIST Mass and Fragment Calculator software [7]. There are no significant peaks at or near this mass in the deconvoluted mass distributions for samples of either SRM 2921a or SRM 2921.

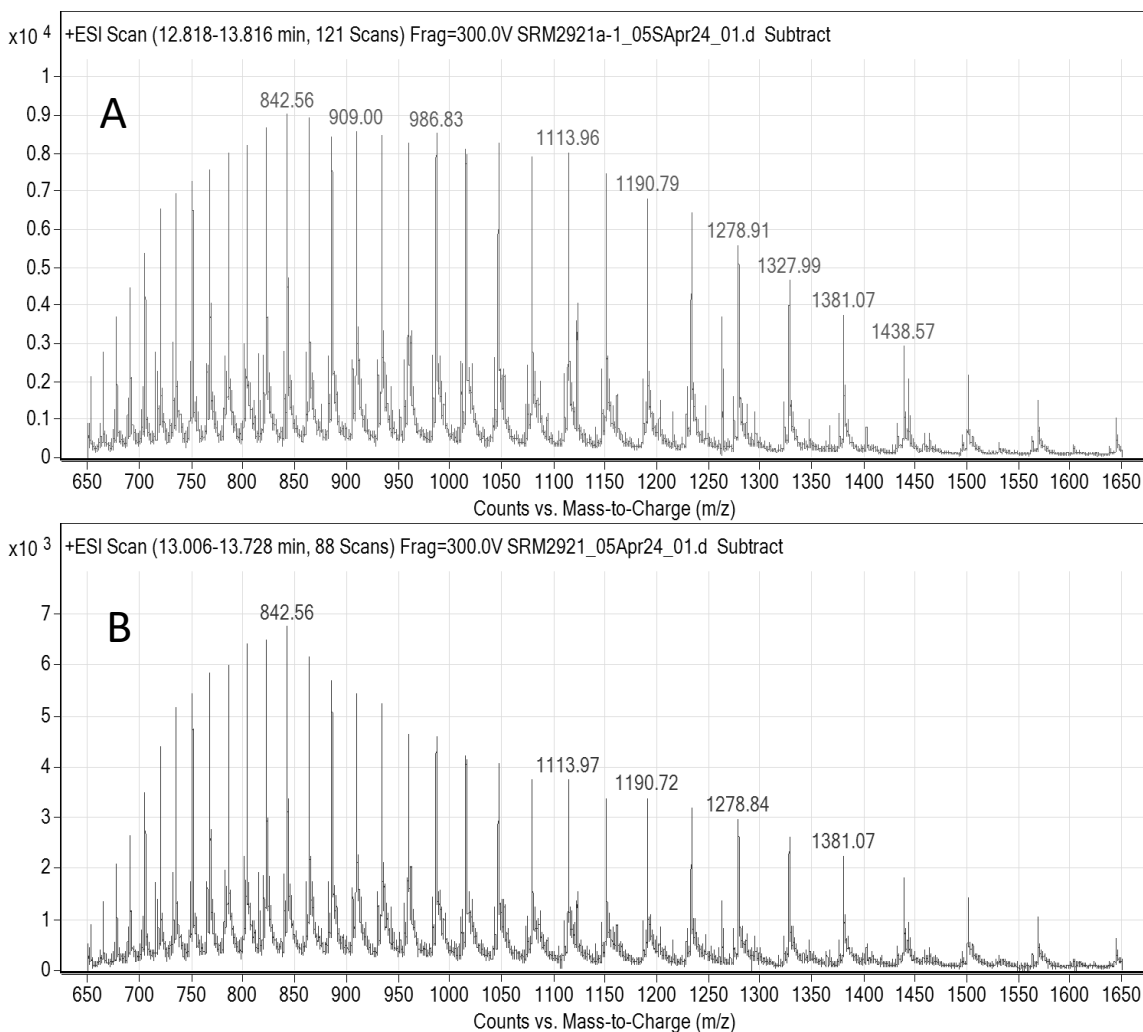


**Figure 2.** Averaged mass spectra from the peak associated with cTnT in A) SRM 2921a, and B) SRM 2921 from Figure 1.

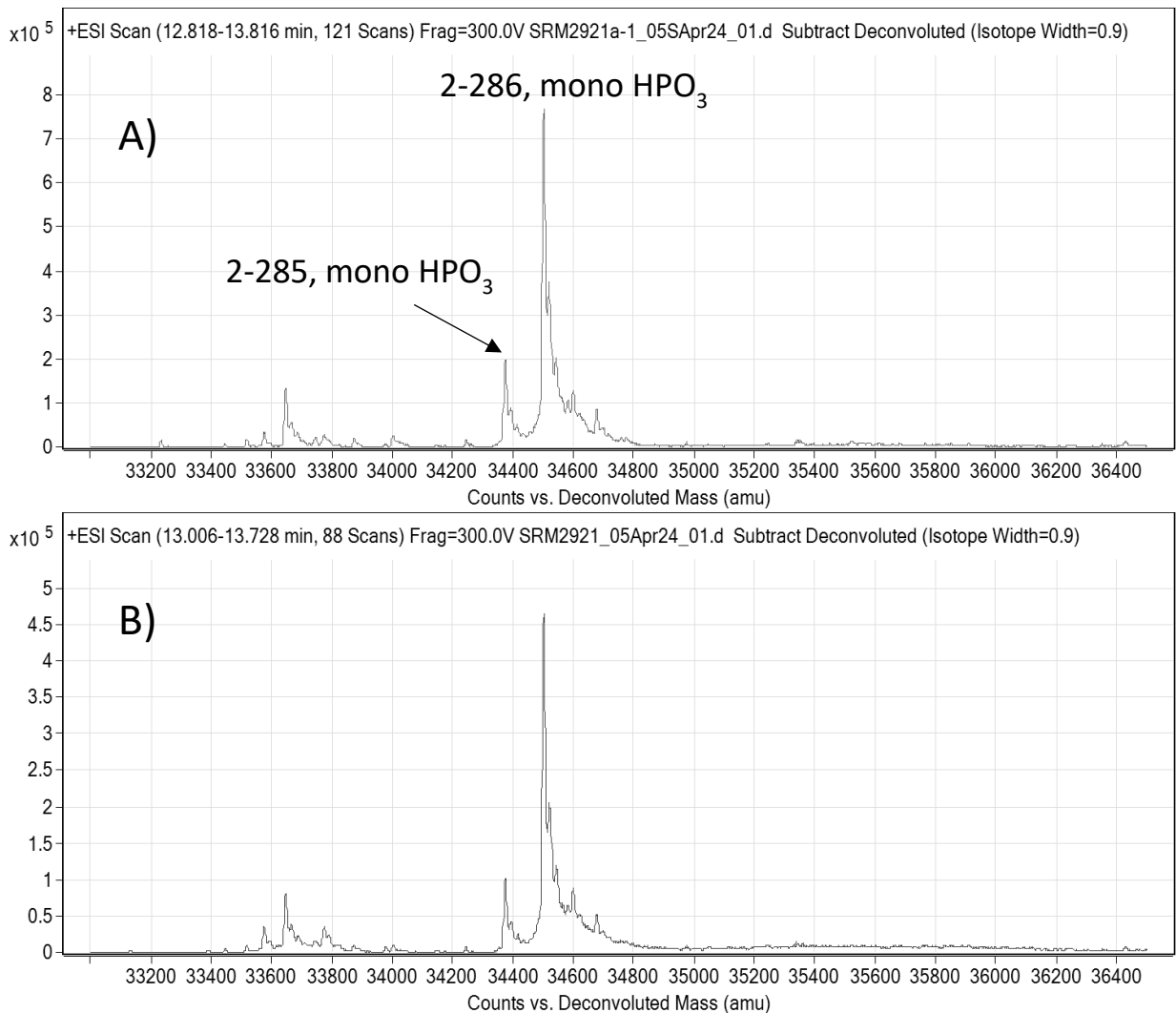


**Figure 3.** Deconvoluted mass distributions of the cTnT peak for A) SRM 2921a and B) SRM 2921. Tentative identifications of cTnT proteoforms of the major masses are assigned to peaks in A). Spectral deconvolution was performed using Agilent MassHunter BioConfirm software.

The most abundant peak in the deconvoluted mass distributions of the first main chromatographic peak for both SRM 2921a and SRM 2921 was observed at approximately 34502 Da, significantly lower than the expected average mass of 35791.9 Da. The tentative assignment of this peak is that of a fragment of cTnT that has a C-terminal “ragged end” missing 12 amino acid residues from the C-terminus and has been singly phosphorylated on one residue (i.e., cTnT 2-286, mono-phosphorylated, calculated average mass = 34502.26). Like most expressed proteins, the N-terminal methionine residue also appears to be excised from cTnT. Based on this assignment, the second most abundant peak in the deconvoluted mass distributions of samples of SRM 2921a and SRM 2921 could be another mono-phosphorylated fragment, missing one additional C-terminal amino acid (i.e., cTnT 2-285, mono-phosphorylated, calculated average mass = 34374.09). The calculated and observed masses for both peak assignments for the

deconvoluted mass distribution of the first main chromatographic peak from samples of SRM 2921a are listed in Table 1.

**Table 1.** Calculated and observed masses for the identified peaks in the deconvoluted mass spectra of cTnT for SRM 2921a

Protein Structure	Calculated Mass <sup>1</sup> , Da	Observed Mass <sup>2</sup> , Da	Mass Difference, Da
cTnT 2-298 (intact cTnT)	35791.90	Not observed	
cTnT 2-286	34422.28	Not observed	
cTnT 2-286, mono-HPO <sub>3</sub>	34502.26	34502.10 ± 0.03	-0.16
cTnI 2-285, mono-HPO <sub>3</sub>	34374.09	34373.65 ± 0.02	-0.44

1 Average mass calculated using the NIST Mass and Fragment Calculator, v2.0

2 The uncertainty expressed here is the standard deviation for mass measurement (N = 6)

In addition to these two tentatively assigned peaks, the deconvoluted mass distributions shown in Figure 3 for the cTnT chromatographic peak of samples from both SRM 2921a and SRM 2921 contain many additional lower-abundance peaks at lower molecular masses. However, these peaks do not appear to originate from cTnT fragments with additional C-terminal amino acid truncations or additional or no phosphorylation based on their observed masses and the masses of calculated fragments. No matches to the observed masses were found for any amino acid cleavages from the N-terminus or combinations of N- and C-terminal fragmentation. It is possible that proteases have removed amino acid residues from an internal portion of the chain. However, because the amino acid sequence of cTnT [6] contains no cysteines, no intra-chain disulfide bonds are possible that could hold the molecule together covalently if there were internal chain cleavage. Under the chromatographic conditions of this analysis, it is unlikely that a non-covalent complex of cTnT fragments would be observed. At this time, the origins of the additional signals in the additional peaks in the deconvoluted spectra for cTnT have not been identified.

Figure 4A shows the mass spectrum averaged from the chromatographic peak eluting at approximately 15 min in the LC-MS analysis of SRM 2921a, the peak assigned to cTnI. Figure 4B shows the averaged mass spectrum from the same chromatographic peak as analyzed in SRM 2921. Both average spectra in Figure 4 show a complex distribution of multiply-charged molecular ions characteristic of a protein. The deconvoluted mass distributions from the averaged spectra in Figure 4 are shown in Figure 5A and Figure 5B for SRM 2921a and SRM 2921, respectively. The identification of peaks in Figures 5A and 5B is based on comparisons of observed masses to calculated average molecular masses for expected cTnI molecular forms and fragments. Table 2 lists calculated and observed masses for the peaks identified in Figure 5. The average masses were calculated from the amino acid sequence of cTnI [8] using the NIST Mass and Fragment Calculator software [7]. Although the amino acid sequence of human cTnI contains two cysteine residues, there is no evidence from the scientific literature that a disulfide bond exists between the two cysteines; therefore, the calculated masses in Table 2 do not factor in a disulfide bond.

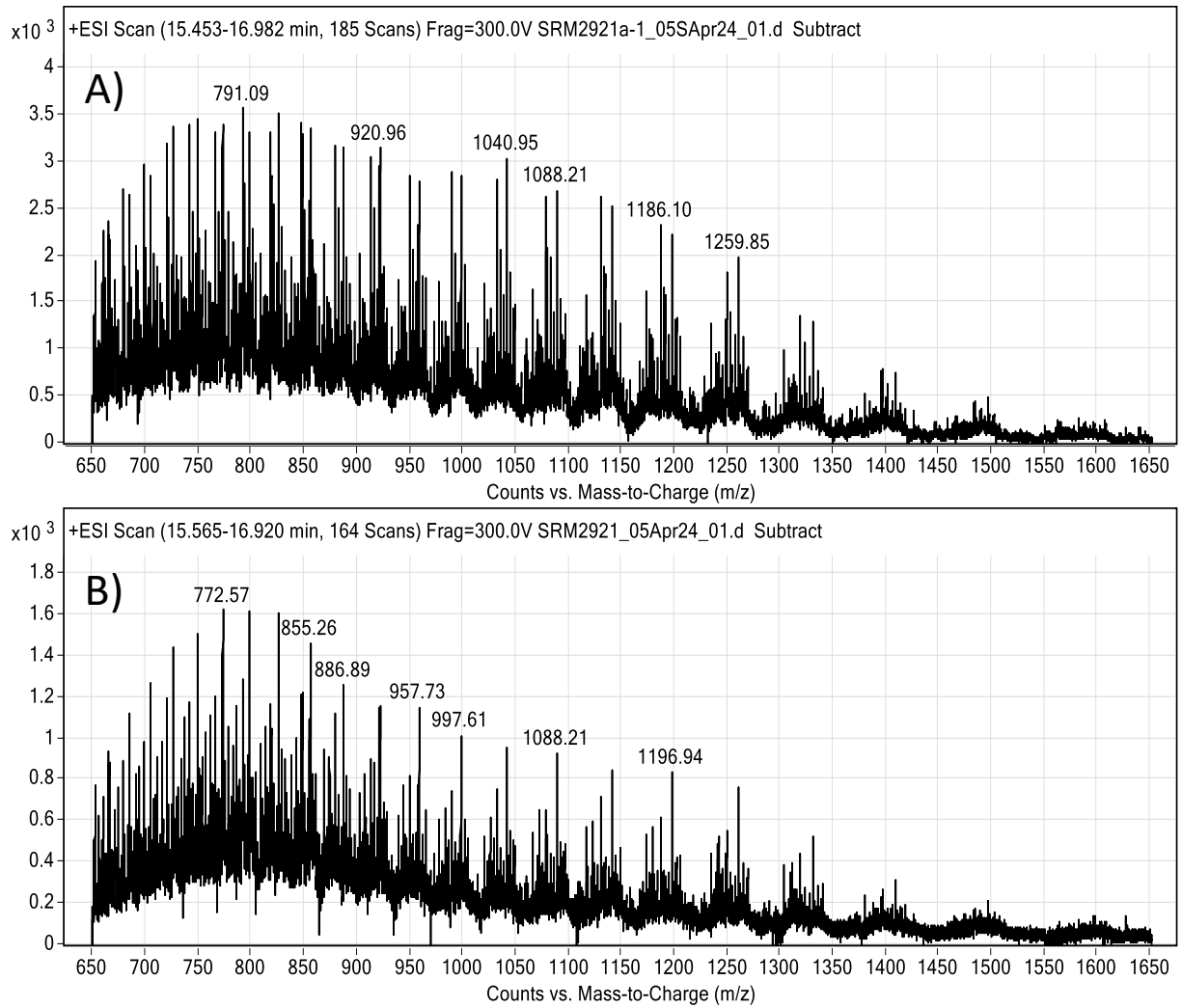


**Figure 4.** Averaged mass spectra from the peak associated with cTnI in A) SRM 2921a, and B) SRM 2921 from Figure 1.

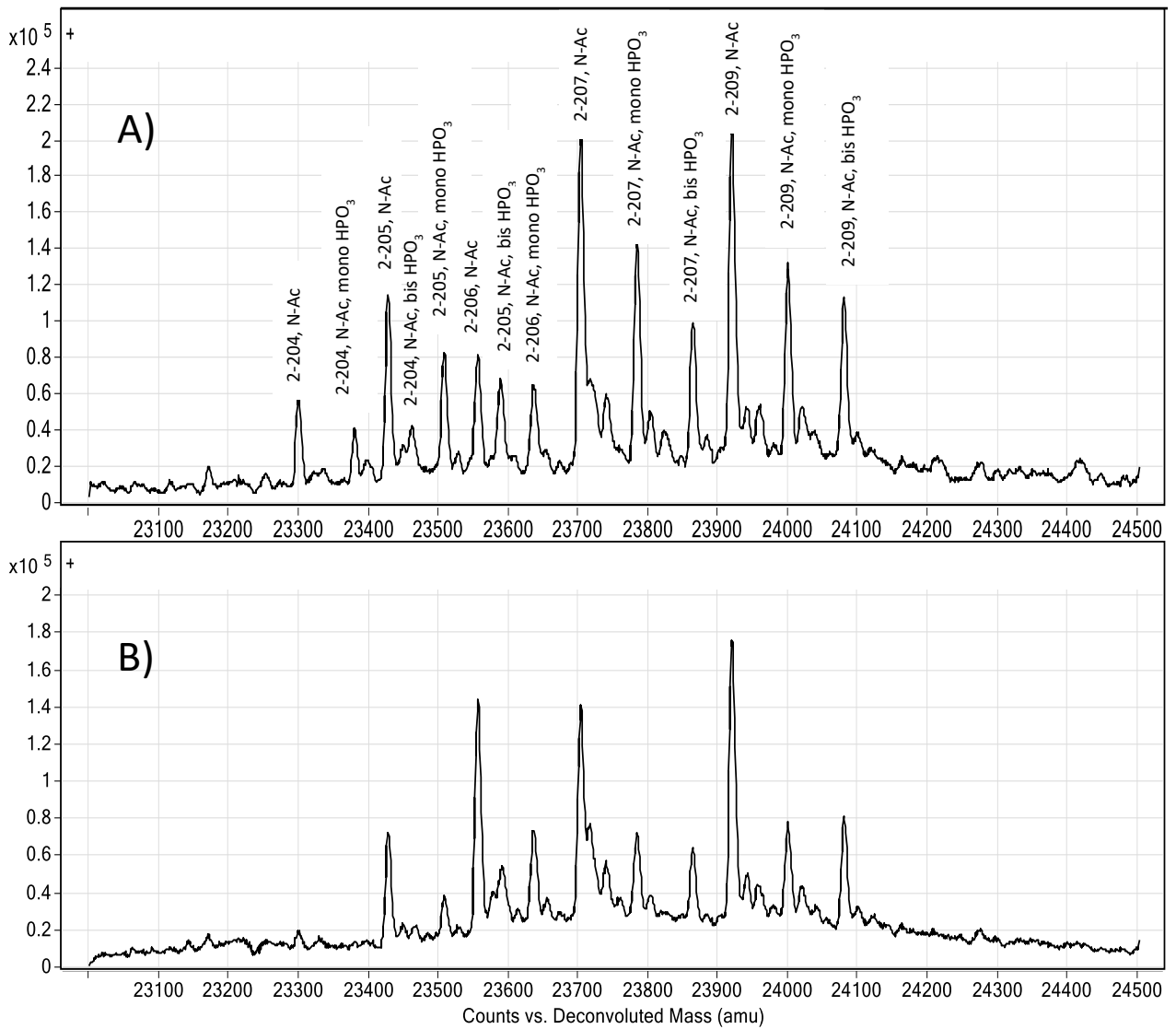


**Figure 5.** Deconvoluted mass distributions of the cTnI peak for A) SRM 2921a and B) SRM 2921. Tentative identifications of cTnI proteoforms of the major masses are assigned to peaks in A). Spectral deconvolution was performed using Agilent MassHunter BioConfirm software.

**Table 2.** Calculated and observed masses for the identified peaks in the deconvoluted mass spectra of cTnI for SRM 2921a.

Protein Structure	Calculated Mass <sup>1</sup> , Da	Observed Mass <sup>2</sup> , Da	Mass Difference, Da
cTnI 2-209, N-Ac, bis-HPO <sub>3</sub>	24078.08	24079.14 ± 0.05	1.05
cTnI 2-209, N-Ac, mono-HPO <sub>3</sub>	23998.10	23999.09 ± 0.02	0.99
cTnI 2-207, N-Ac	23918.12	23919.27 ± 0.03	1.15
cTnI 2-207, N-Ac, bis-HPO <sub>3</sub>	23861.89	23863.34 ± 0.04	1.45
cTnI 2-209, N-Ac, mono-HPO <sub>3</sub>	23781.91	23783.29 ± 0.04	1.38
cTnI 2-207, N-Ac	23701.93	23703.05 ± 0.06	1.12
cTnI 2-206, N-Ac, bis-HPO <sub>3</sub>	23714.71	Not observed	
cTnI 2-206, N-Ac, mono-HPO <sub>3</sub>	23634.73	23636.29 ± 0.33	1.56
cTnI 2-206, N-Ac	23554.75	23555.53 ± 0.15	1.83
cTnI 2-205, N-Ac, bis-HPO <sub>3</sub>	23586.54	23588.37 ± 0.14	0.78
cTnI 2-205, N-Ac, mono-HPO <sub>3</sub>	23506.56	23507.58 ± 0.09	1.02
cTnI 2-205, N-Ac	23426.28	23427.54 ± 0.05	2.12
cTnI 2-204, N-Ac, bis-HPO <sub>3</sub>	23458.37	23460.49 ± 0.74	1.26
cTnI 2-204, N-Ac, mono-HPO <sub>3</sub>	23378.39	23379.47 ± 0.06	1.08
cTnI 2-204, N-Ac	23298.41	23299.61 ± 0.07	1.20

1 Average mass calculated using the NIST Mass and Fragment Calculator, v2.0

2 The uncertainty expressed here is the standard deviation for mass measurement (N = 6)

In both SRM 2921a and SRM 2921, LC-MS analysis indicates that there is intact cTnI present that is both N-acetylated and both mono- and bis-phosphorylated. Like the cTnT subunit, the N-terminal methionine residue also appears to be excised from cTnI. There also appears to be significant amounts of truncation of C-terminal amino acids. There does appear to be more C-terminal fragmentation in samples from SRM 2921a as compared to samples from SRM 2921. Comparing the observed and calculated masses for these tentative peak assignments in Table 2 shows a consistent mass difference of approximately 1 Da with the observed masses consistently higher than the calculated masses. A possible explanation for a consistent mass difference is a bias in calibration. Because the deconvoluted masses are derived from multiply-charged peaks, a slight mass bias in the measurement of a multiply-charged peak would be multiplied by the charge number of that peak to determine the deconvoluted mass. It should be noted that the same mass calibration that produced the masses listed in Table 2 for cTnI was also applied to yield the masses in Table 1 for cTnT (as well as Table 3, below). A possible chemical explanation for the observed mass difference is a deamidation of an asparagine or glutamine residue, which would add approximately 0.98 Da to the observed mass; cTnI contains several asparagine and glutamine residues.

Figure 6A shows the mass spectrum averaged from the chromatographic peak eluting at approximately 19 min in the TIC shown in Figure 1A for the LC-MS analysis of SRM 2921a. For comparison, Figure 6B shows the average spectrum for the same peak from the LC-MS analysis of SRM 2921. Upon deconvolution of the average spectra, the mass distributions for the two spectra in Figure 6 are shown in Figure 7. The peak identified in the mass distribution in Figure 7A for SRM 2921a is tentatively assigned to the intact cTnC molecule with an N-acetylation. Table 3 lists the calculated and observed mass for this peak assignment. The average masses were calculated from the amino acid sequence of cTnC [9] using the NIST Mass and Fragment Calculator software [7]. While human cTnC contains two cysteine residues, there is no evidence that they are linked by a disulfide bond; therefore, the calculated average mass listed in Table 3 does not account for the presence of a disulfide bond. As with the peaks assigned for cTnI, the most prominent peak signal observed for cTnC is approximately 1 Da higher than its calculated mass. This mass difference could be due to a calibration bias or to a chemical modification like deamidation of asparagine or glutamine residues; both amino acids are part of the amino acid sequence of cTnC.

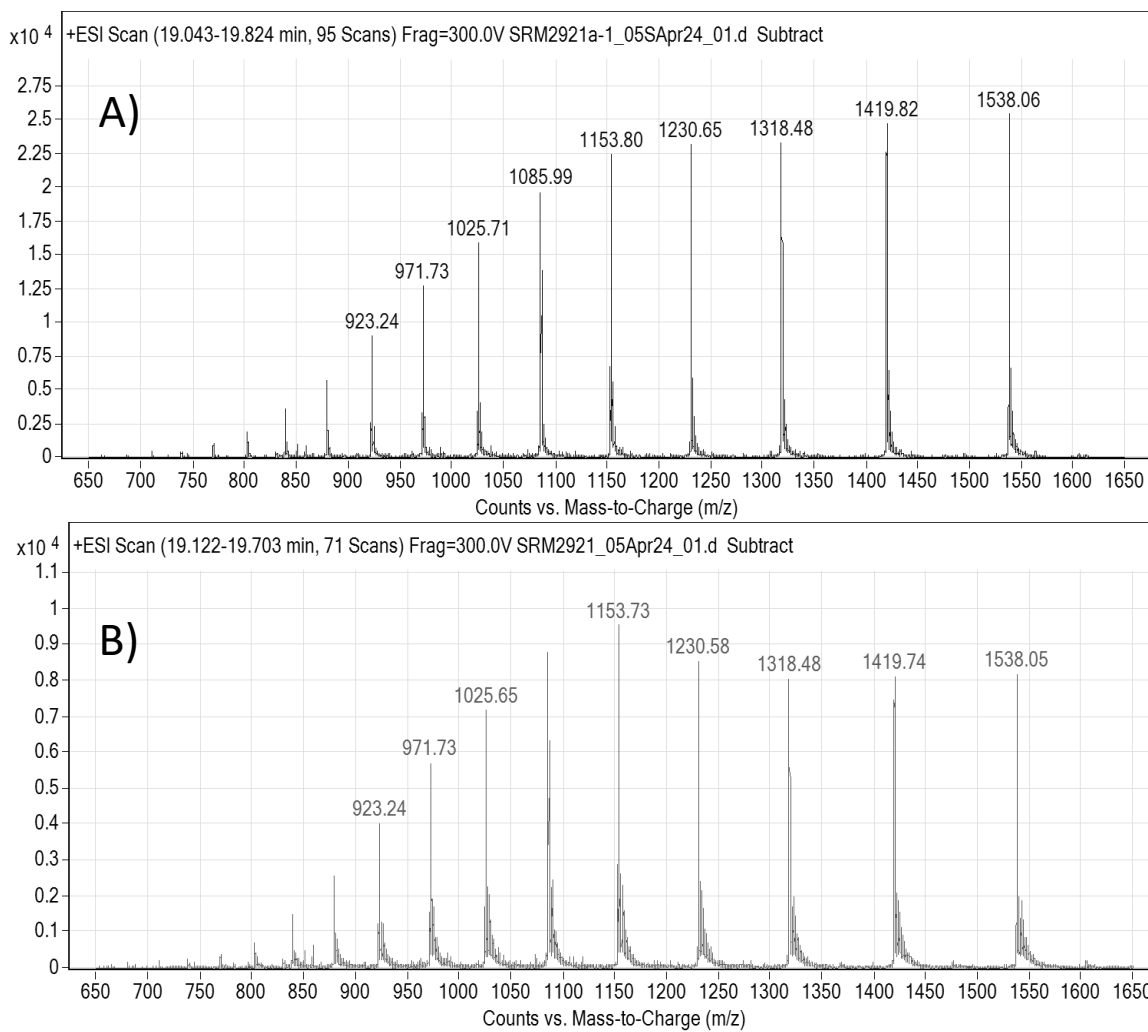


**Figure 6.** Averaged mass spectra from the peak associated with cTnC in A) SRM 2921a, and B) SRM 2921 from Figure 1.

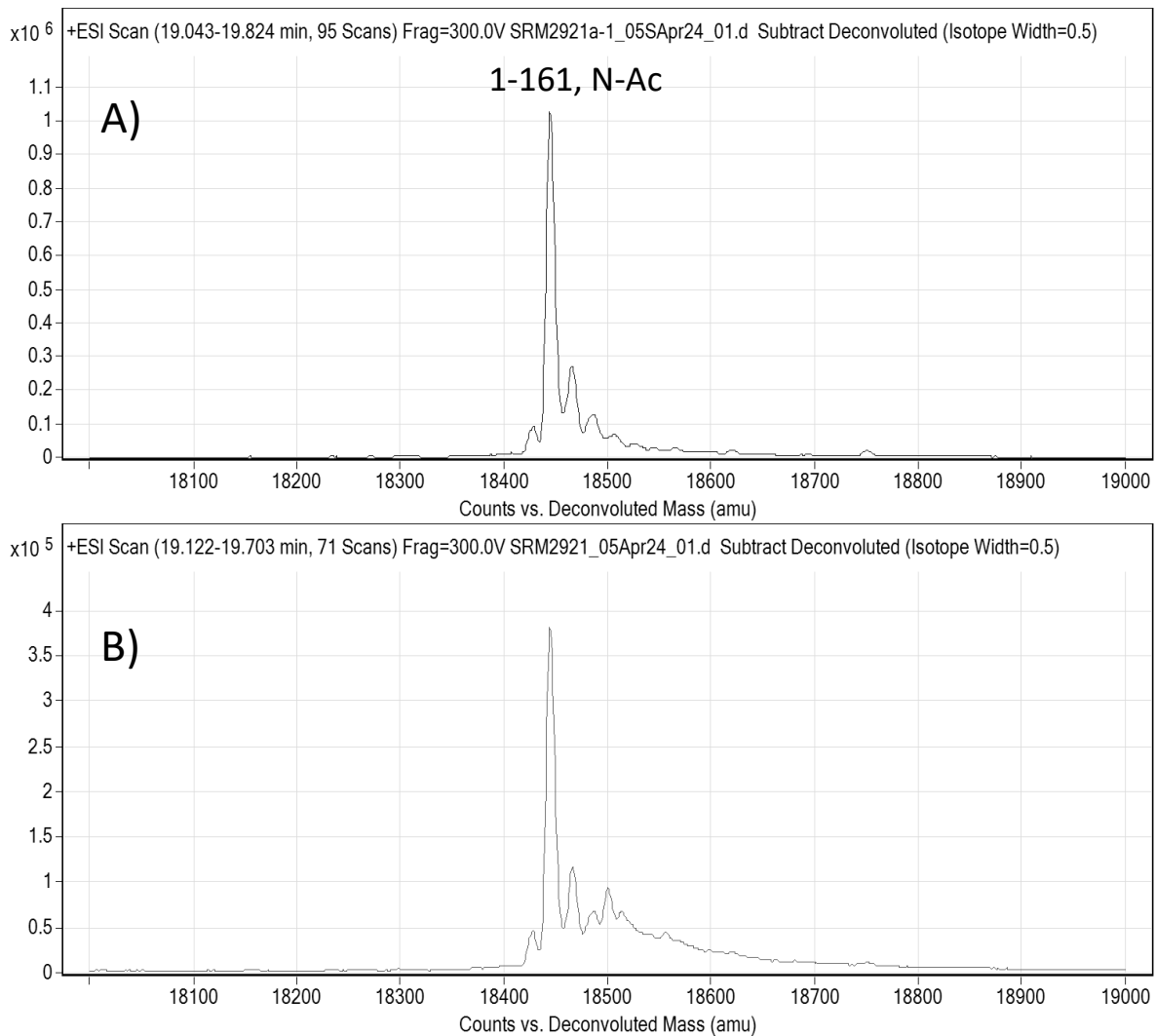


**Figure 7.** Deconvoluted mass distributions of the cTnC peak for A) SRM 2921a and B) SRM 2921. Tentative identification of the cTnC proteoform is assigned to the peak with the highest signal abundance in A). Spectral deconvolution was performed using Agilent MassHunter BioConfirm software.

**Table 3.** Calculated and observed masses for the identified peak in the deconvoluted mass spectra of cTnC for SRM 2921a.

Protein Structure	Calculated Mass <sup>1</sup> , Da	Observed Mass <sup>2</sup> , Da	Mass Difference, Da
cTnC 1-161, N-Ac	18444.40	18445.26 ± 0.06	0.86

1 Average mass calculated using the NIST Mass and Fragment Calculator, v2.0

2 The uncertainty expressed here is the standard deviation for mass measurement (N = 6)

Of the two prominent peaks labeled as “contaminants” in the TICs shown in Figure 1, the peak(s) between the cTnT and cTnI peaks appear to be the result of several molecular species capable of forming multiply-charged ions, presumably proteins or protein fragments. Figure 8A shows the deconvoluted mass distribution from a peak eluting at approximately 14.3 min from one LC-MS analysis of SRM 2921a. The prominent masses in this mass distribution are all lower than those of cTnT, cTnI, and cTnC, leaving the possibility that these proteins are fragments of any one of these proteins or all of them. These protein species could also potentially be impurities from the process of extracting the troponin complex used to prepare SRM 2921a from human heart tissue. For comparison, Figure 8B shows the deconvoluted mass distribution from the spectra of the same peak area from the analysis of SRM 2921. There are similarities and differences in the mass distributions shown in Figure 8A and Figure 8B, indicating that similarities and differences exist within the protein impurities in SRM 2921a and SRM 2921.

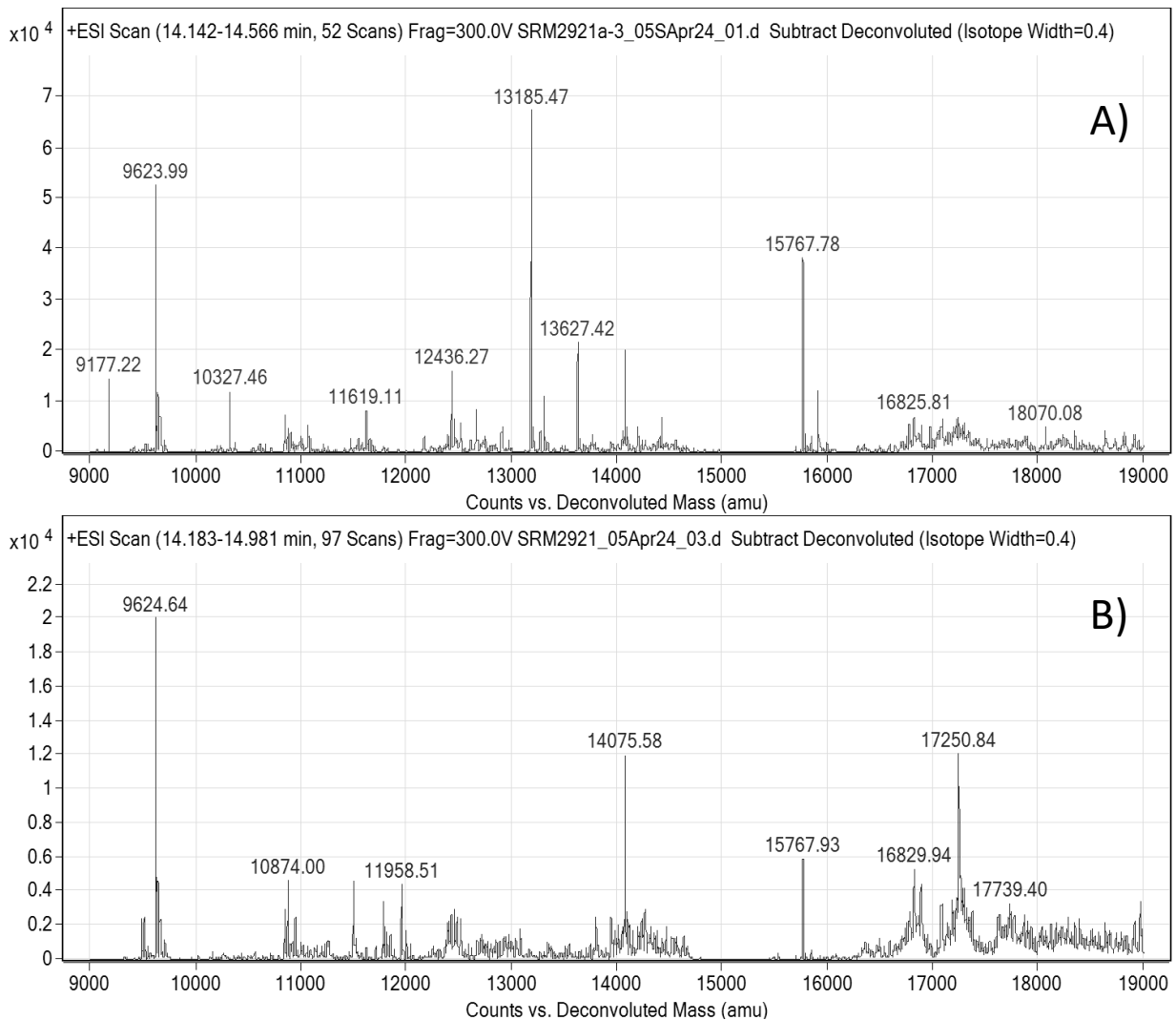


**Figure 8.** Deconvoluted mass distributions of the peak designated as “Impurity 1” in Figure 1 for A) SRM 2921a, and B) SRM 2921.

Figure 9A and Figure 9B show the spectra averaged from the scans under the peak eluting at approximately 22.7 min from the LC-MS analysis of SRM 2921a and SRM 2921, respectively, which is labeled “Impurity 2” in Figure 1. The peaks shown in Figure 9 are not the typical multiply-charged ion series that is observed for proteins. The  $m/z$  spacing between the peaks is consistently the same, approximately 44. This mass difference between ions suggests a polymeric material with a polyethylene backbone. Polyethylene-based surfactants are frequently used in the extraction and purification of proteins. They generate strong signals using electrospray ionization and, therefore, even small amounts can produce strong LC-MS chromatographic peaks. The differences in the distribution of peaks in Figure 9A and Figure 9B may reflect differences in the polymer distributions of surfactant impurities present in SRM 2921a and SRM 2921.

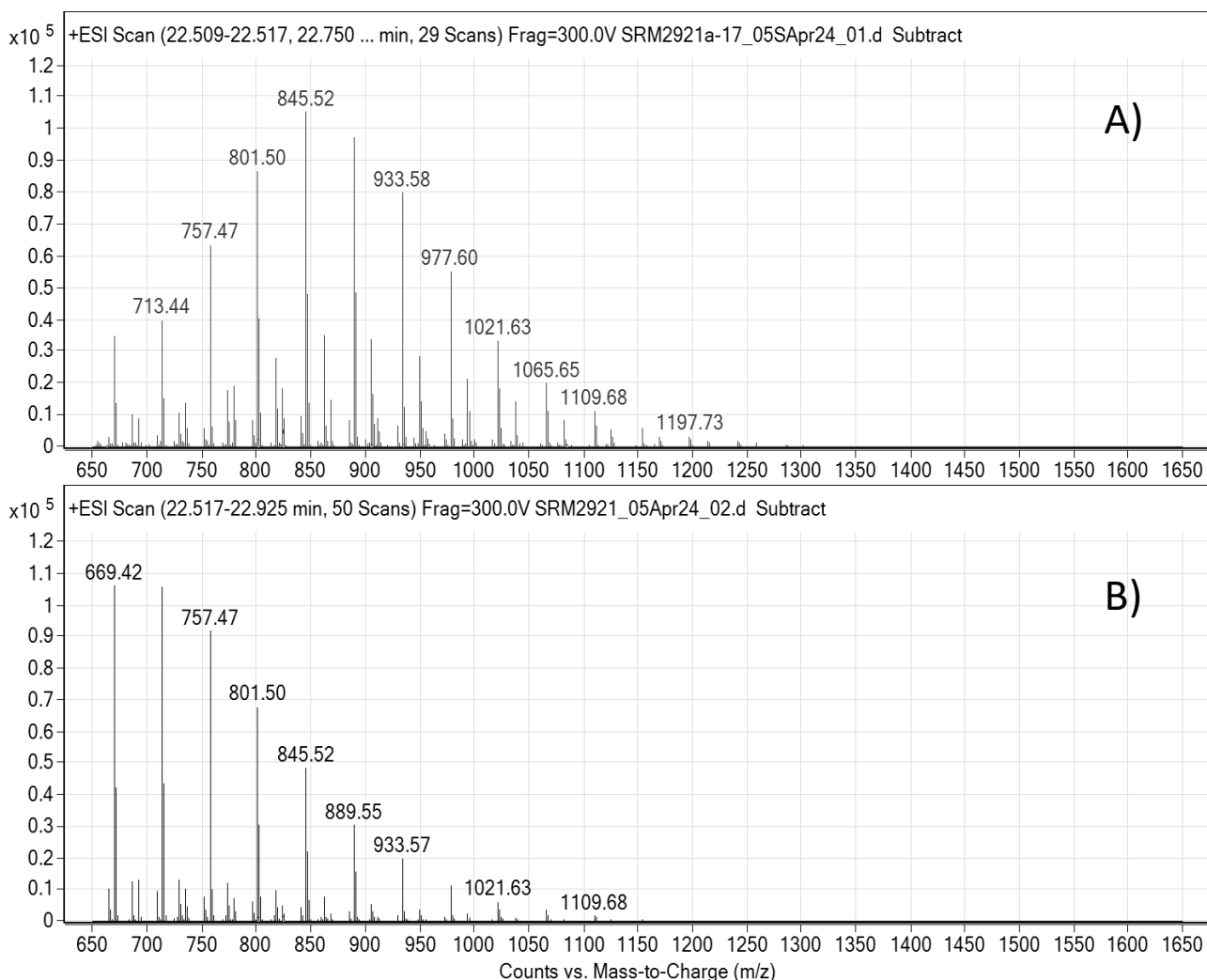


**Figure 9.** Averaged mass spectra from the peak designated as “Impurity 2” in Figure 1 for A) SRM 2921a, and B) SRM 2921.

## 5. SRM 2921A Certification Plan and Method Development

In the initial certification plan, a commercial preparation of purified human cTnI was to be used to establish calibration for an LC-MS measurement of the intact cTnI subunit in SRM 2921A. The amount-of-substance concentration of calibration solutions prepared from purified human cTnI would be determined using quantitative amino acid analysis using isotope dilution LC-MS/MS after hydrolysis of the cTnI into its constituent amino acids. Quantitative amino acid analysis of protein solutions requires either highly purified protein solutions or the quantitative assessment of impurities in the protein that may yield amino acids.

To carry out certification, purified human cTnI was obtained from HyTest Ltd., the company that was the source of the human troponin complex for both SRM 2921 and SRM 2921a (although the material from SRM 2921a was purchased from Fitzgerald Industries International, Fitzgerald obtained it originally from HyTest, according to a representative from HyTest). Unfortunately, once calibrators were prepared using the Fitzgerald/HyTest purified human cTnI, it was discovered that both the purity of this material and the molecular mass distribution of the purified human cTnI differed significantly from those of the cTnI in SRM 2921a. Figure 10 compares the LC-MS data from the purified human cTnI to the data from SRM 2921a.

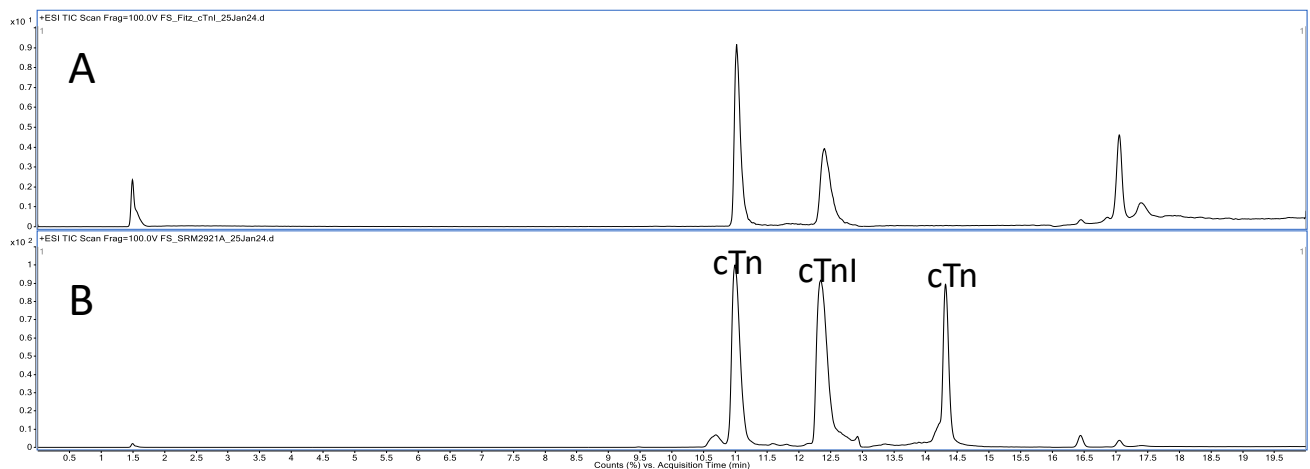


**Figure 10.** Total ion chromatogram (TIC) from the LC-MS analysis of A) purified cTnI, and B) SRM 2921a

In Figure 10B, peaks from the three troponin subunits are seen as the most abundant signals in the total ion chromatographs (scanning  $m/z$  750 to  $m/z$  1500) from the LC-MS analysis using the Agilent 6460 triple quadrupole mass spectrometer. In Figure 10B, it is observed that the cTnT subunit elutes first, followed by cTnI and then cTnC. In Figure 10A, the total ion chromatograph from the LC-MS analysis of the purified cTnI material obtained to prepare calibrators, there is clearly a significant amount of cTnT and a strong late-eluting peak whose spectra suggest a polymeric material rather than a protein.

While Figure 10A shows that the purified cTnI material does have a strong peak eluting at approximately the same retention time as the cTnI peak in SRM 2921a, the mass spectra underlying both peaks are not similar. Figure 11 compares the averaged spectra from the peaks associated with cTnI in both the purified cTnI material (Figure 11A) and SRM 2921a (Figure 11B).

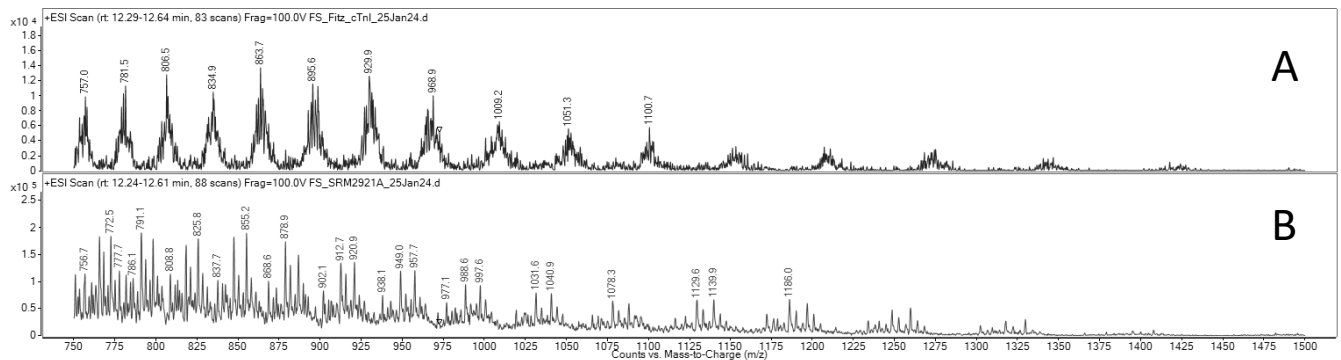


**Figure 11.** Averaged spectra from the peak associated with cTnI in A) the purified cTnI material, and B) SRM 2921a from Figure 10.

The presence of other proteins at significantly high concentrations relative to that of cTnI means that the concentration of cTnI in this purified preparation could not be value-assigned using quantitative amino acid analysis. The other proteins in the preparation would yield amino acids that would be indistinguishable from those from cTnI. There would be no way to accurately quantify the amino acids originating from cTnI and, therefore, no way to accurately quantify the concentration of cTnI in a preparation with significant amounts of other proteins.

The decision was made not to procure and evaluate purified human cTnI from other vendors as materials obtained from HyTest in the past have always been very high quality; if the purified material from HyTest did not have sufficient purity to be used as a calibrator, finding a better material was unlikely.

An alternative certification plan was devised that used SRM 2921 to prepare calibrators for the value assignment of the cTnI concentration in SRM 2921a. The certification method used LC-MS with selected ion monitoring (SIM) to assign cTnI concentration from calibrants (SRM 2921) to sample (SRM 2921a). The SIM analysis used signals from multiply-charged ion peaks, such as those shown in Figure 4, from intact troponin complex protein subunits separated by reversed-phase liquid chromatography.

## 5.1. Evaluating Mobile Phase Additives

Reversed-phase liquid chromatographic separations of intact proteins and large peptides frequently use trifluoroacetic acid (TFA) as a mobile phase additive. TFA provides sharp peaks for protein separations and has been shown to improve the recovery of proteins from the chromatography stationary phase [10] [11]. Unfortunately, TFA is also known to quench signals when using electrospray ionization in positive ion LC-MS analysis [12], sometimes as much as several orders of magnitude compared to other acidic modifiers like acetic or formic acid. It has been reported in the literature that using formic acid in the mobile phase at levels of 0.5 % (v/v) or above can improve chromatographic peak shape [13] without the signal quenching observed when TFA is used.

Figure 12 compares the chromatographic separation of the troponin subunits in SRM 2921a using 0.5 % (v/v) formic acid (Figure 12A) and 0.1 % TFA (v/v) (Figure 12B). To collect the total ion chromatograph data shown in Figure 12, the mass spectrometer was scanned from  $m/z$  750 to  $m/z$  1500. It should be noted that the peak areas for the three troponin subunits in Figure 12B are approximately 1000 times lower than the corresponding peak areas in Figure 12A, reflecting the significant loss of positive ion electrospray signal when TFA is used. Also, note that the signal from proteins is preferentially quenched in electrospray ionization by the presence of TFA in the mobile phase, but the suspected detergent impurity peak, eluting at approximately 13.25 min in Figure 12B, does not appear to be significantly impacted.

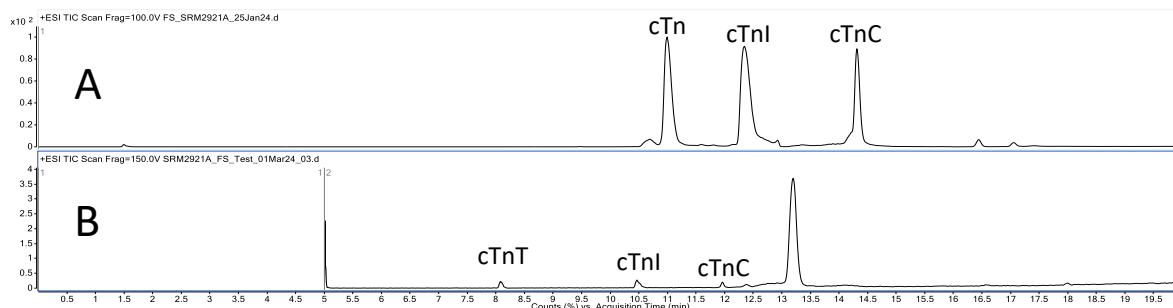


**Figure 12.** Comparison of the chromatographic separation of dilutions of SRM 2921a using A) 0.5 % (v/v) formic acid and B) 0.1 % (v/v) trifluoroacetic acid as mobile phase additive.

While 0.5 % (v/v) formic acid provided much higher signals than when TFA was used, replicate analysis of samples showed poor peak area reproducibility with formic acid, varying, at times, by as much as a factor of 40 (See Table 4). The data in Table 4, from replicate injection of two samples prepared from dilutions of SRM 2921A, demonstrate the repeatability of peak area determinations using different mobile phases (which were also used as sample diluent). While the peak areas from LC-MS using SIM are significantly larger when 0.5 % formic acid is used as the mobile phase additive as compared to 0.1 % TFA, peak areas show significant variability between replicate injections with formic acid.

**Table 4.** Comparison of LC-MS peak areas for replication injections of samples prepared from SRM 2921A using 0.5 % formic acid and 0.1 % TFA as mobile phase additive.

	<b>0.5 % Formic Acid</b>	<b>0.1 % TFA</b>
<b>Injection</b>	<b>Peak Area</b>	<b>Peak Area</b>
1	742588	207866
2	8934699	213613
3	8373145	215480
4	813230	216436
5	8817134	217626
6	8615853	213710
<b>Average</b>	<b>6049442</b>	<b>214122</b>
<b>SD</b>	<b>4087823</b>	<b>3436</b>
<b>CV</b>	<b>67.6 %</b>	<b>1.6 %</b>

Because the planned method of certification relies on the precision of peak area reproducibility but does not require high measurement sensitivity, separation using formic acid as the mobile phase additive was ruled out despite the greater signal abundance.

## 5.2. SIM Method Development

LC-MS of the intact protein subunits of the human troponin complex was combined with SIM to quantify the cTnI concentration in SRM 2921a using calibration solutions prepared from SRM 2921. Three m/z values were chosen for the SIM method that correspond to the m/z values of adjacent  $(M+nH)^{n+}$  ions in the multiply-charged ion distribution of the intact protein. Figure 13 compares the averaged mass spectra from the cTnI peaks in A) SRM 2921a and B) SRM 2921 using full-scan mode on the Agilent 6460 triple quadrupole mass spectrometer.

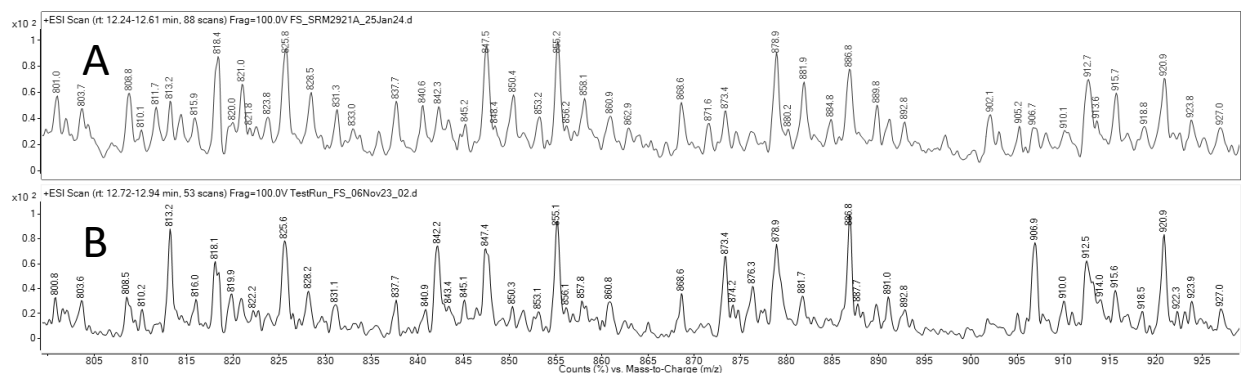


**Figure 13.** Averaged mass spectra from the cTnI chromatographic peak in the LC-MS analysis of A) SRM 2921a and B) SRM 2921.

The peaks observed centered at approximately  $m/z$  825.7,  $m/z$  855.1, and  $m/z$  886.8 in the averaged mass spectra for both SRM 2921a and SRM 2921 correspond to the  $(M+29H)^{29+}$ ,  $(M+28H)^{28+}$ , and  $(M+27H)^{27+}$  cTnI molecular ion peaks, respectively, for the N-acetylated cTnI 2-207 proteoform shown in Figure 5A. This proteoform was chosen as the focus of the measurement because it is one of the proteoforms with the most complete cTnI amino acid sequence observed with the least number of post-translational modifications. Additionally, the three peaks from the N-acetylated cTnI 2-207 proteoform are frequently the most abundant molecular ion peaks in the averaged mass spectra of cTnI. They were selected as the peaks to be monitored in SIM mode of the LC-MS method for quantification. Due to slight variability in the relative intensities of these three peaks from run to run, the integrated intensities (i.e., SIM peak areas) from all three were combined for data analysis.

Preliminary quantitative analysis indicated that the concentration of SRM 2921a was higher than that of SRM 2921. Therefore, to prepare calibrators with concentrations that bracket the approximate cTnI concentration of SRM 2921a, dilutions of SRM 2921a were necessary to prepare analytical samples, and one dilution of SRM 2921 and undiluted SRM 2921 were necessary to create bracketing calibrators. The dilution scheme is outlined in Figure 14.

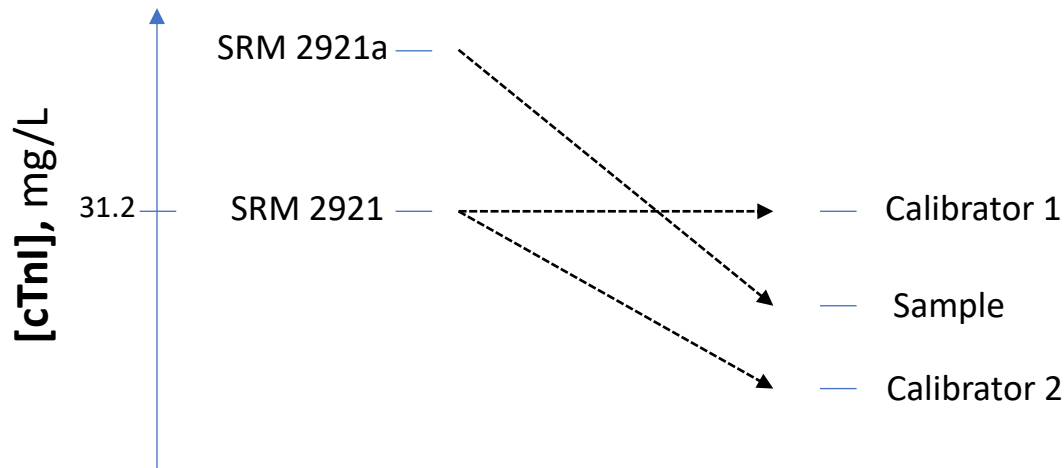


**Figure 14.** Dilution scheme for the quantification of cTnI concentration in SRM 2921a using calibrators prepared from SRM 2921.

A dilution scheme that minimized the magnitude of all dilutions was chosen to reduce the variability that can happen from adsorptive losses when protein concentrations become low and are in contact with surfaces like pipette tips and sample tubes. Therefore, the calibrator 1 solutions for bracketing calibration were prepared without dilution by directly transferring SRM 2921 to autosampler vial inserts (after thawing and gentle mixing). The calibrator 2 solutions had minimal dilution.

A comparison of diluents was performed to evaluate how the choice of diluent impacts the reproducibility of LC-MS peak areas. The diluents compared were the buffer used to prepare SRM 2921a (20 mmol/L Tris, 150 mmol/L NaCl, 5 mmol/L CaCl<sub>2</sub>, pH 7.57) and mobile phase A (0.1 % TFA in water). Table 5 compares the LC-MS peak area reproducibility from samples of SRM 2921a prepared gravimetrically with different diluents. Because the first injection of protein samples frequently has a peak area that noticeably differs from subsequent replicate injections of the same sample, the data from the first of the six injections was not used to evaluate reproducibility.

**Table 5.** Evaluation of the dilution buffer used to prepare samples and calibrators for the certification of SRM 2921a by LC-MS. Note that averages and standard deviations were calculated using the last 5 LC-MS runs in each set of 6 replicate injections.

Sample	Injection	Diluent	Combined SIM Peak Area
2921A-30-1	1	buffer	165418
2921A-30-1	2	buffer	181229
2921A-30-1	3	buffer	180255
2921A-30-1	4	buffer	180624
2921A-30-1	5	buffer	180822
2921A-30-1	6	buffer	179042
<b>AVG =</b>			180394
<b>SD =</b>			834
<b>CV =</b>			0.46 %
2921A-30-2	1	mobile phase A	207866
2921A-30-2	2	mobile phase A	213613
2921A-30-2	3	mobile phase A	215480
2921A-30-2	4	mobile phase A	216436
2921A-30-2	5	mobile phase A	217626
2921A-30-2	6	mobile phase A	213710
<b>AVG =</b>			215373
<b>SD =</b>			1738
<b>CV =</b>			0.81 %

The reproducibility of LC-MS peak areas was excellent regardless of the diluent. The peak areas from the sample produced using mobile phase A were slightly higher because the gravimetric dilution factor was slightly less than that of the other sample. The buffer used to prepare SRM 2921a was chosen as the diluent used to prepare samples and the low-concentration calibrators. Using the SRM 2921a buffer as diluent also matched the matrices of samples to both calibrators, given that one of the calibrators used was undiluted SRM 2921.

### 5.3. Optimization of Chromatographic Column Clean-up

Because no internal standard will be used for this certification method, it is important to verify that sample-to-sample carryover during the LC-MS/MS measurement is minimized. Two of the main sources of sample-to-sample carryover in the reversed-phase chromatography of proteins are carryover in the autosampler (on the injection needle and needle seals) and the chromatographic column (from incomplete protein elution). These sources of potential sample-to-sample protein carryover can be addressed through more extensive needle-washing cycles with appropriate wash solvents and through mobile phase gradients run without protein sample injection (i.e., blank gradients).

Peak area reproducibility was examined for replicate injections of samples prepared from SRM 2921a using a standard needle wash and with additional needle and column washes between sample injections. Table 6 compares the sample worklists for this peak area reproducibility assessment.

**Table 6.** Comparison of sample worklists for the evaluation of needle and column washes on peak area reproducibility.

<b>No Wash Worklist:</b>	<b>Worklist with Washes:</b>
Wash	Wash
Sample	Sample
Sample	Wash
Sample	Sample
Sample	Wash
Sample	Sample
Sample	Wash
Wash	Sample
	Wash
	Sample
	Wash
	Sample
	Wash

The peak area reproducibility of replicate injections of a typical calibration sample is shown in Table 7 for replicate injections without a column and injector wash between injections and with between-injection washes. The data shown in Table 7 demonstrates that column and injector washes between sample injections are important to achieve measurement repeatability. Therefore, in the certification of SRM 2921a, column and injector wash runs were performed between every injection of sample or calibrant. Appendix C lists the experimental conditions for the final SIM LC-MS method. The LC-MS conditions for the needle and column wash method are listed in Appendix D.

**Table 7.** Comparison of the peak area reproducibility of replicate injections of a calibrator prepared from SRM 2921 with and without injector needle washes between injections. The sample used for replicate analysis was a blend of two previously prepared calibration solutions.

<b>Sample</b>	<b>Analysis</b>	<b>Combined Peak Area</b>
Cal 1 + 2 Blend	No wash run between injections	155335
Cal 1 + 2 Blend	No wash run between injections	150988
Cal 1 + 2 Blend	No wash run between injections	143960
Cal 1 + 2 Blend	No wash run between injections	147215
Cal 1 + 2 Blend	No wash run between injections	136267
	CV =	4.9 %
Cal 1 + 2 Blend	Wash run between injections	144689
Cal 1 + 2 Blend	Wash run between injections	143690
Cal 1 + 2 Blend	Wash run between injections	142993
Cal 1 + 2 Blend	Wash run between injections	139716
Cal 1 + 2 Blend	Wash run between injections	139388
	CV =	1.7 %

## 6. Certification Measurements of SRM 2921a by LC-MS using Selected Ion Monitoring

Preliminary measurements made during method development indicated that the highest level of reproducibility would be obtained with column and needle washing between every data collection run. Consequently, only four samples of SRM 2921a were measured in each measurement set, along with two sets of bracketing calibrants prepared from SRM 2921 and blanks to keep the total measurement time for each set of samples and calibrants within a reasonable time of a few days. Each of these was measured in triplicate (i.e., triplicate injections of each sample) on each measurement set. Five of these sets were run in total, with samples and calibrants for each set being prepared immediately before the LC-MS/MS measurement. Samples of SRM 2921a were taken from boxes across the fill range so that the homogeneity of the SRM 2921a lot could be assessed.

Figure 15 shows examples of the total ion chromatogram from the LC-MS analysis, using SIM scanning mode, for A) a calibration sample prepared by diluting SRM 2921, and B) a dilution of SRM 2921a. The total ion chromatograms shown in Figure 15 are the sum of the signals from the three  $m/z$  values measured in the SIM scanning method.

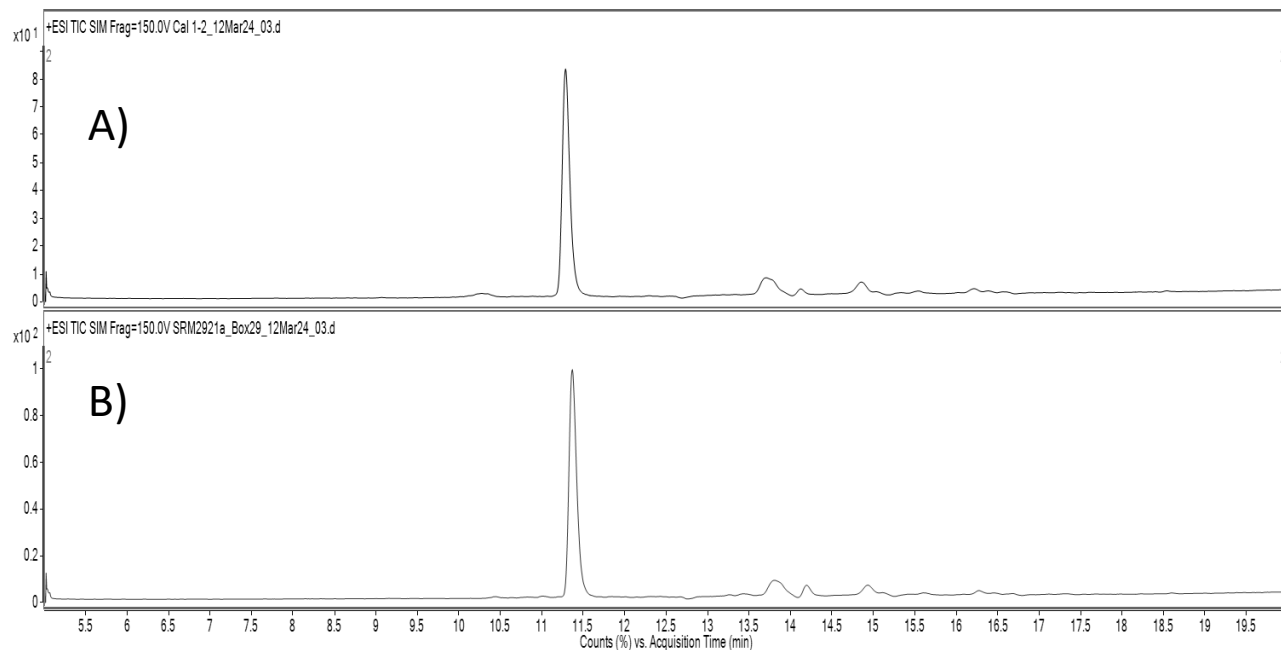


**Figure 15.** Total ion chromatogram from the LC-MS analysis in SIM mode of A) calibration sample prepared from SRM 2921, and B) sample prepared from SRM 2921a.

An instrument worklist from one set of LC-MS analyses is shown in Appendix E.

Calibration curves were prepared from each set of bracketing calibrants on each day of analysis. The concentration of each calibrant was calculated from the certified cTnI concentration value of SRM 2921 and the gravimetric dilution factor unique to each prepared calibration solution. Peak areas from the LC-MS total ion chromatograms were obtained using Agilent Qualitative Analysis with automatic peak area integration using default software settings. A typical bracketing calibration curve is shown in Figure 16.

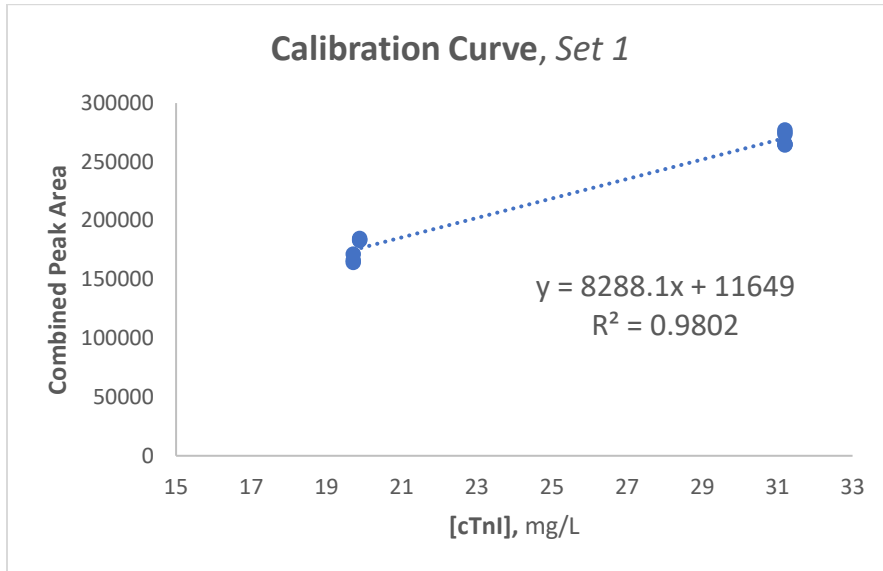


**Figure 16.** Calibration curve from the bracketing calibration for certification set 1.

Table 8 lists the slope, intercepts, and  $R^2$  values from the calibration curves for all five sets of certification analysis. The calibration curve slopes show a high degree of variability between sets. The source of this between-set variability isn't apparent from an examination of the data. When the calibration curves from all five sets of certification samples are overlaid (see Figure 17 below), there is considerable variability in the peak area signals from both bracketing calibrants, even for the higher concentration calibrant, the undiluted SRM 2921. The high degree of between-set signal variability for the high-level calibrant indicates that sample preparation was unlikely to be a source of the variability, as the use of the high-level calibrant involved essentially no sample preparation.

**Table 8.** Calibration curve parameters from the five sets of calibration data.

Set	Slope	Intercept	$R^2$
1	8288.1	+11649	0.9802
2	6062.2	+69059	0.9833
3	10218	-1046.6	0.9959
4	9833.3	+20201	0.9792
5	9471.2	+29165	0.9590

### 6.1. Certification Measurement Results for SRM 2921a

Table 9 lists the averaged measured SRM 2921a cTnI concentration results from each measurement set. All measurement results from the five sets of analysis are listed in Appendix F. Raw measurement and sample preparation data for the five sets are listed in Appendix G.

**Table 9.** Averaged measurement results for the cTnI concentration in SRM 2921a. The standard deviations listed are from the measured concentration values and do not reflect the expanded uncertainty

Set	Average [cTnI], mg/L	Standard Deviation, mg/L
1	132.73	2.93
2	140.13	3.17
3	134.02	2.16
4	143.03	5.95
5	149.39	4.07

The standard deviation of the average of each measurement set listed in Table 9 does not include a complete uncertainty budget.

## 7. Statistical Evaluation of SRM 2921a Certification Data

The experimental data used for the analysis of SRM 2921a includes five sets of repeated calibration experiments. For each of the five measurement sets, SRM 2921 and a dilution of SRM 2921 were used as bracketing calibrants. This SRM is assumed to have a concentration of 31.2 mg/L, with a standard uncertainty of 1.4 mg/L. Two levels of this calibrant are used: 1) the original level of 31.2 mg/L, and a diluted level, approximately 20 mg/L (which varies slightly for each set of certification samples).

LC-MS was used to produce a mass spectrogram of each SRM 2921a sample and SRM 2921 calibrant, and software was used to determine the total peak area of the signal from cTnI. Effectively, each sample or calibrant has an associated peak area (measured in triplicate), and each total peak area, as a function of troponin-I concentration, is assumed to be linear. Thus, for new samples, troponin concentration is estimated by first computing the peak area via LC-MS, and then back calculating based on the estimated functional relationship of the calibrants whose concentration is known (at least up to some uncertainty). A visual display of the data can be seen in Figure 17 below. As is evident from Figure 17, there are some differences in the calibrant function (and thus the back-calculated cTnI concentrations) across the various measurement sets. To address this, we incorporate hierarchical models, which assume that each set has its own calibration function, which is drawn from some underlying probability distribution (whose parameters are estimated by the statistical inference procedure outlined in the following section).

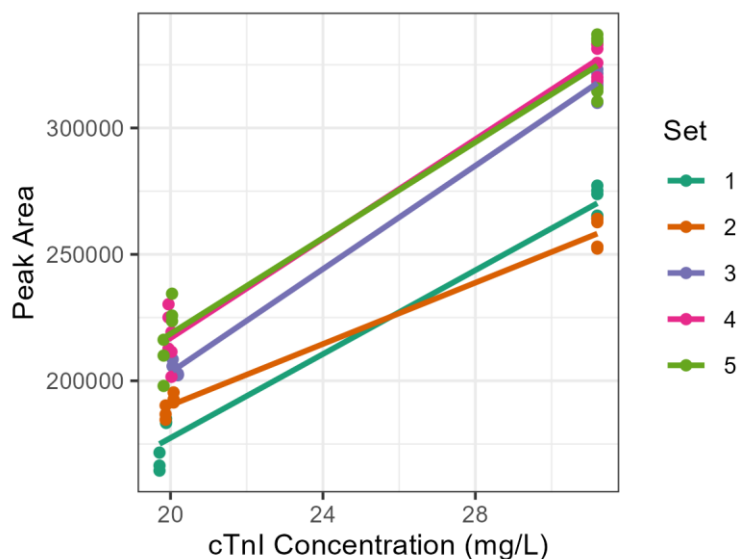


**Figure 17.** Data used for calibration functions. Points represent LC-MS data (peak areas) from calibrants prepared from SRM 2921, and diagonal lines represent estimated calibration functions.

## 7.1. Statistical Modeling

To carry out inference testing on the concentration for SRM 2921a, we model the data generation process as a hierarchical Bayesian model. An introduction to such models and their utility in the context of metrology can be found in [14]. For this analysis, the model is composed of two parts: one to model the calibration functions, and another to back-calculate and combine the observed values for SRM 2921a. We model the measurements of the calibrator, SRM 2921, as a linear model with varying slopes and varying intercepts, to consider clear differences in slope and intercept between the five measurement sets. Second, we use the observed peak areas for samples prepared from SRM 2921a, for each set, to estimate the cTnl concentration for each measurement of SRM 2921a. These back-calculated values have uncertainties due to 1) measurement error of the peak intensities (assumed to be independent and identically distributed, i.e., Gaussian) from the LC-MS measurement, and 2) uncertainty in the slope and intercept for the given set. Finally, once we obtain estimates and uncertainties of the cTnl concentration for each sample, we can then combine these measurements using a random effects model accounting for the individual samples' uncertainties.

The multi-stage model below provides a general schematic for the varying-slopes, varying-intercepts model used for modeling the SRM 2921 measurements. We leave out a few details for clarity (such as scaling the error terms with the magnitude of the cTnl concentration), but these details can be seen in the associated stan model files, in Appendix H.

$$\begin{aligned}
 \mu, \beta_1, \beta_2, \sigma, \sigma_{b_0}, \sigma_{b_1} &\sim \pi \\
 \delta &\sim N(31.2, 1.4^2) \\
 b_{i,0} &\sim N(\beta_0, \sigma_{b_0}^2), \quad i = 1, \dots, 5 \\
 b_{i,1} &\sim N(\beta_1, \sigma_{b_1}^2), \quad i = 1, \dots, 5 \\
 r_{ij} &\sim N(b_{0,i} + b_{1,i}(s_{ij} + \delta), \sigma^2), \quad j = 1, \dots, J
 \end{aligned}$$

One unique feature of this model is the single (unknown) error term,  $\delta$ , which accounts for the uncertainty in SRM 2921. This error is modeled as a Gaussian random variable with standard deviation 0.7 mg/L, based on the reported expanded uncertainty of 1.4 mg/L from the original certificate. This uncertainty is shared across all cTnl calibrator concentration values prepared from SRM 2921.

For the peak area measurements of SRM 2921a,  $r_{ij}'$ , we use the inverse of the calibration function, while considering the uncertainties in each set's slope and intercept. That is,

$$s_{ij}' = \frac{r_{ij}' - b_{0,i}}{b_{1,i}}$$

To be clear,  $r_{ij}'$  is an observed peak area value, and the  $b$  terms in the numerator and denominator above are random variables which have (posterior) probability distributions derived from the previous step. Thus, each  $s_{ij}'$  has its own posterior distribution, which can then all be combined into a model for SRM 2921a. This model is as follows:

$$\begin{aligned}\mu, \sigma, \sigma_{day} &\sim \pi \\ \alpha_i &\sim N(0, \sigma_{day}^2) \\ s_{ij}' &\sim N(\mu + \alpha_i, \sigma^2 + u_{s_{ij}}^2)\end{aligned}$$

This model takes into account sources of variability such as: uncertainty due to the calibration procedure, uncertainty in the cTnl concentration of SRM 2921, between-set variability, and between-sample variability. From these sources, we can estimate the mean cTnl concentration for 2921a, along with its associated standard and expanded uncertainties.

## 8. Certification Measurement Results

The estimates and variability in cTnI concentration of the SRM 2921a samples are shown in Figure 18. The estimate of the grand mean,  $\mu$ , is indicated as the solid vertical black line, while the standard uncertainties and expanded uncertainties are shown as dashed and dotted lines, respectively. The results depicted as points centered on horizontal lines are derived from fitting the hierarchical calibration model described above and represent estimates and uncertainties for the 2921a samples. The uncertainties take into account uncertainty in the slopes and intercepts for each of the calibration curves, uncertainty in the calibrator SRM 2921, as well as within-set variability. These estimates and uncertainties are taken into account for the mean estimate and uncertainty provided in the measurement claim.

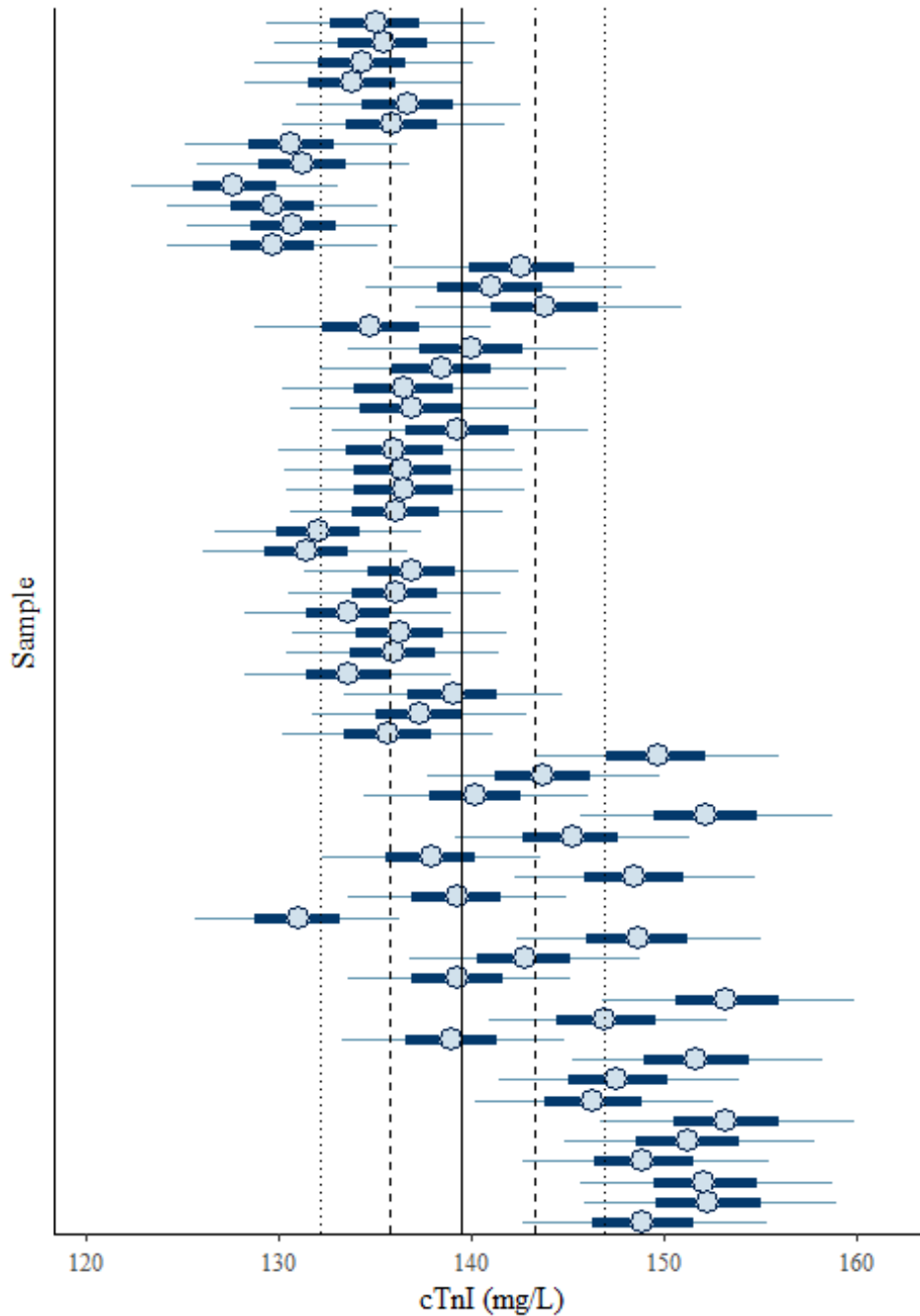


**Figure 18.** Posteriors for individual SRM 2921a samples. Thin lines represent 95 % posterior intervals, thick blue lines represent 80 % posterior intervals, and points indicate the median of each posterior distribution. The solid vertical line represents the overall mean estimate, while dashed and dotted lines represent +/- one standard uncertainty and one expanded uncertainty, respectively.

The key parameter estimates of the statistical modeling are given below. Each row represents a different parameter of interest for the model.  $\mu$  represents the overall central estimate of cTnI for the 2921a samples, while  $\sigma_{set}$  and  $\sigma_{within\_set}$  represent

between-set and within-set variability, respectively. *sigma\_calibrant* is an estimate of the uncertainty for each measurement, due to the calibration experiment. *beta0* and *beta1* provide estimates and uncertainties of the linear calibration function (using standardized values for the peak areas), while *tau\_b0* and *tau\_b1* represent between-set variability for the slopes and intercepts. More details on the modeling results, as well as the Stan model files, can be found in Appendix H.

**Table 10.** Model results.

Parameter	Est	u(Est)
<i>mu</i>	139.55	3.73
<i>sigma_set</i>	7.49	2.89
<i>sigma_within_set</i>	1.43	0.81
<i>sigma_calibrant</i>	3.64	0.28
<i>beta0</i>	-4.04	0.24
<i>beta1</i>	0.16	0.02
<i>tau_b0</i>	0.48	0.26
<i>tau_b1</i>	0.04	0.02

From Table 10 above, we see that the dominant sources of variability appear to be due to variability between sets and the calibration experimental process (which includes the uncertainty of SRM 2921). The sample-to-sample variability within a single day appears to be negligible, relative to the other sources. The expanded uncertainty of the mean, which is approximately 7.5 mg/L, accounts for all these sources. (Note that the uncertainty in the mean does not equal the root sum of squares of all sources of uncertainty, which would represent a prediction interval corresponding to the variability of individual replicates for the specific process carried out at NIST.)

## 9. SRM 2921a Measurement Claim

Below, in Table 12, is the measurement claim for the mean cTnI concentration in SRM 2921a:

**Table 11.** Measurement claim for cTnI concentration in SRM 2921a

Estimate (mg/L)	$u$ (mg/L)	$U$ (mg/L)	$k$	DoF
139.55	3.73	7.39	1.98	121

In Table 12, the *Estimate* column provides an estimate for the mean cTnI concentration for SRM 2921a, while the  $u$  and  $U$  represent the standard and expanded uncertainties, respectively. The expansion factor is given as  $k = 1.98$ , representing an uncertainty interval at a 95 % level. The associated degrees of freedom are 121. (Note: Using numbers of degrees of freedom is justifiable only when the probability distribution that characterizes measurement uncertainty is (approximately) a Student's  $t$  distribution. The GUM [15] assumes that it is always so, based on clauses G.2-G.4. However, these clauses reflect mostly wishful thinking. The advent of modern methods for uncertainty evaluation, including Monte Carlo methods (such as the Monte Carlo Markov Chain, which is used for this analysis), has opened the door to a realistic characterization of uncertainty using probability distributions. In many cases, these distributions are not even close to a Student's  $t$ ).

## **10. Measurement Traceability**

The certified concentration of cTnl in SRM 2921a is metrologically traceable to the International System of Units (SI) through calibration with NIST SRM 2921 [16].

## 11. Homogeneity Assessment

For a protein solution in a vial, such as SRM 2921a, it is generally assumed that there are no significant within-vial homogeneity issues if a protein solution is sufficiently mixed, and the proteins are all soluble and remain soluble. However, there is a possibility of between-vial homogeneity problems for a large lot of vials, such as those produced for SRM 2921a. There may be changes to the bulk protein solution in the time it takes to fill all vials in a large lot.

A stratified measurement approach was taken for the certification measurements to assess any homogeneity issues across the vial fill order for SRM 2921a. Each certification measurement set contained vials pulled from boxes at the beginning, middle, and end of the fill order for SRM 2921a. Each box contained 100 filled vials. Box 1 was the first box filled; box 29 was the last.

Figure 19 shows a plot of the measured concentration of cTnI in each vial versus the box number from which the vial was pulled. Figure 19 shows the possibility of a decrease in the cTnI concentration of SRM 2921a as the fill box number increases. The large scatter in the cTnI concentration data in Figure 19 results from between-set measurement variability. This is illustrated in Figure 20 where the same data is shown across the 5 sets. The between-set measurement variability appears to be larger than any variability due to homogeneity issues across the lot. Additionally, a two-way ANOVA model with box and set treated as factors does not indicate that the boxes differ statistically (Table 13). Consequently, the SRM 2921a vial lot seems sufficiently homogeneous relative to the uncertainty of the certified cTnI concentration. Because a stratified sampling plan was used for certification measurements, a plan that sampled across the entire vial fill order, the overall uncertainty of the certified cTnI concentration of SRM 2921a does incorporate an uncertainty component for inhomogeneity.

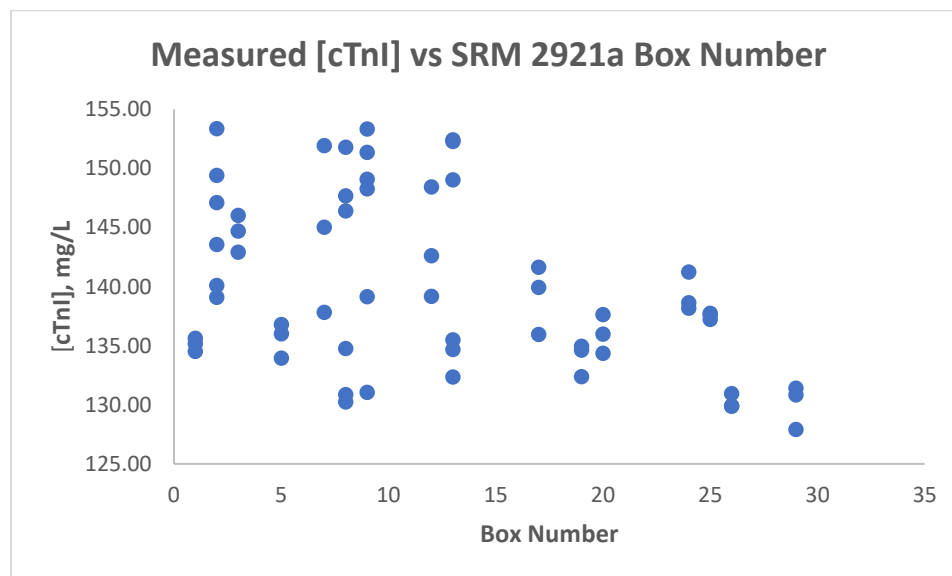


**Figure 19.** The measured concentration of cTnI in SRM 2921a versus the box number from which the sample was chosen.

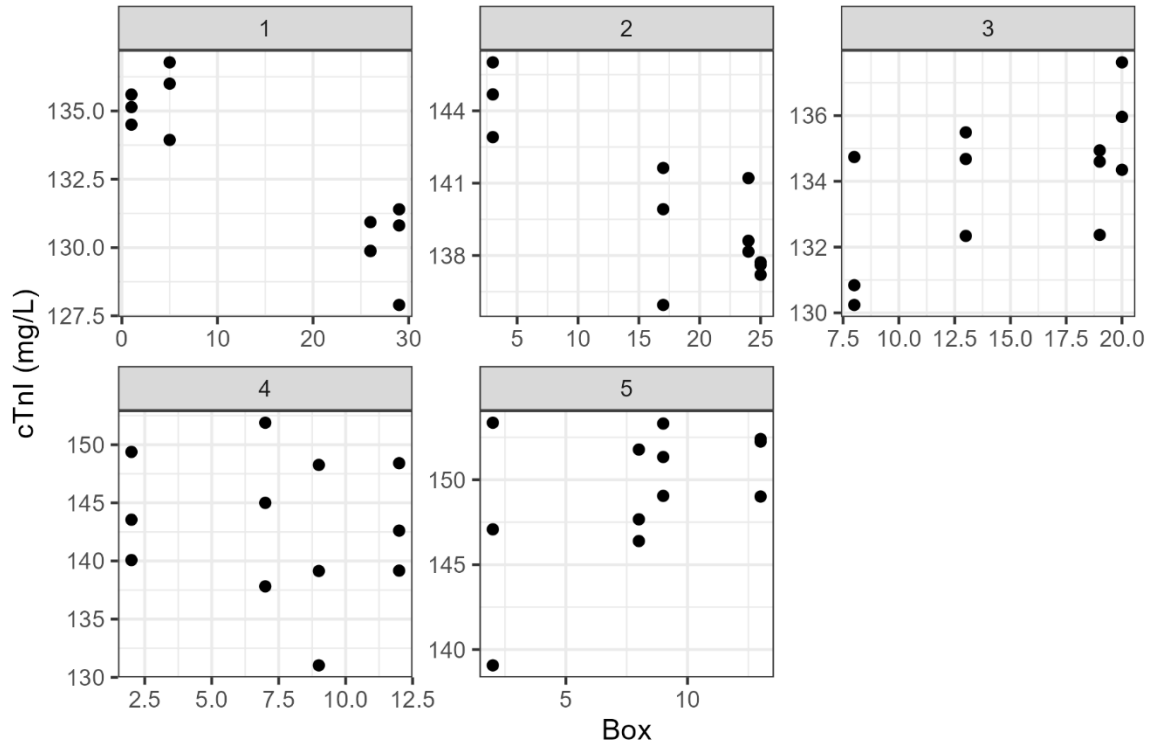


**Figure 20.** The measured concentration of cTnl in SRM 2921a versus the box number from which the sample was chosen, separated by measurement set.

**Table 12.** ANOVA model results for fitting set and box as a function of cTnl.

	Df	Sum Sq	Mean Sq	F value	p
Set	4	2232.055	558.0138	38.6759	1.45E-13
Box	13	221.3018	17.02322	1.179878	0.326635
Residuals	42	605.9738	14.42795		

## 12. References

- [1] Katrukha I (2013) Human cardiac troponin complex. Structure and functions. *Biochemistry* 78(13):1447. <https://doi.org/10.1134/S0006297913130063>.
- [2] Brush J, Kaul S, Krumholz H (2016) Troponin Testing for Clinicians. *Journal of the American College of Cardiology* 68(21):2365. <https://doi.org/10.1016/j.jacc.2016.08.066>.
- [3] Hong J, Chatila KF, John JJ, Thakker RA, Kassem H (2023) Insights on the Etiologies of Chronically Elevated Troponin. *Current Problems in Cardiology* 48(8):101204. <https://doi.org/10.1016/j.cpcardiol.2022.101204>.
- [4] Jarolim P (2015) High sensitivity cardiac troponin assays in the clinical laboratories. *Clinical Chemistry and Laboratory Medicine* 53(5):635. <https://doi.org/10.1515/cclm-2014-0565>.
- [5] Karady J, Mayrhofer T, Ferencik M, Hoffmann U, et al. (2024) Agreement among high-sensitivity cardiac troponin assays and non-invasive testing, clinical outcomes, and quality-of-care outcomes based on the 2020 European Society of Cardiology Guidelines. *European Heart Journal. Acute Cardiovascular Care* 13(1):15. <https://doi.org/10.1093/ehjacc/zuad138>.
- [6] UniProt (2026) UniProt database entry for P45379 - TNNT2\_HUMAN. Available at <https://www.uniprot.org/uniprotkb/P45379/entry>.
- [7] National Institute of Standards and Technology (2025) NIST Mass and Fragment Calculator Software. Available at <https://www.nist.gov/services-resources/software/nist-mass-and-fragment-calculator-software>.
- [8] UniProt (2026) UniProt database entry for P19429 - TNNT3\_HUMAN. Available at <https://www.uniprot.org/uniprotkb/P19429/entry>.
- [9] UniProt (2026) UniProt database entry for P63316 - TNNT1\_HUMAN. Available at <https://www.uniprot.org/uniprotkb/P63316/entry>.
- [10] McCalley D (2004) Effect of buffer on peak shape of peptides in reversed-phase high performance liquid chromatography. *Journal of Chromatography A* 1038(1-2):77. <https://doi.org/10.1016/j.chroma.2004.03.038>.
- [11] Bobaly B, Fekete J (2015) Recovery of proteins affected by mobile phase trifluoroacetic acid concentration in reversed-phase chromatography. *Journal of Chromatographic Science* 53(7):1078. <https://doi.org/10.1093/chromsci/bmu169>.

- [12] Eshraghi J, Singh SK (1993) Factors affecting electrospray ionization of effluents containing trifluoroacetic acid for high-performance liquid chromatography/mass spectrometry. *Analytical Chemistry* 65(23):3528. <https://doi.org/10.1021/ac00071a035>.
- [13] Huber CP (1999) Evaluation of volatile eluents and electrolytes for high-performance liquid chromatography-electrospray ionization mass spectrometry and capillary electrophoresis-electrospray ionization mass spectrometry of proteins. *Journal of Chromatography A* 849(1):161. [https://doi.org/10.1016/s0021-9673\(99\)00532-4](https://doi.org/10.1016/s0021-9673(99)00532-4).
- [14] Meija J, Bodnar O, Possolo A (2023) Ode to Bayesian methods in metrology. *Metrologia* 60(5):052001. <https://doi.org/10.1088/1681-7575/acf66b>.
- [15] Bureau International des Poids et Mesures (2008) Evaluation of measurements data - Guide to the expression of uncertainty in measurement. (BIPM, Sèvres), JCGM 100:2008.
- [16] SRM 2921; Human Cardiac Troponin Complex; National Institute of Standards and Technology; U.S. Department of Commerce: Gaithersburg, MD (24 May 2023). Available at [https://shop.nist.gov/ccrz\\_ProductDetails?sku=2921](https://shop.nist.gov/ccrz_ProductDetails?sku=2921).

## Appendix A. Fitzgerald Industries Certificate of Analysis



Antibodies and Antigens  
are in Our Blood.

Fitzgerald Industries International  
Suite 1A North, 30 Sudbury Road  
Acton, MA 01720, USA  
Tel: 978.371.6446  
Fax: 978.371.2266

www.fitzgerald-fii.com  
Email: antibodies@fitzgerald-fii.com

### Certificate of Analysis Antigen Data Sheet

**Product:** Troponin Complex protein

**Catalog #:** 30R-AT033                      **Grade :** High Purity  
**Lot #:** A16100704                      **Purity:**

**Source:** Human heart tissue

**Concentration:** Troponin I: 1.14mg/ml; Troponin T: 1.16mg/ml; Troponin C: 1.01mg/ml. Total content based on Troponin I content. Ratio of components in complex IT/C: 1/0.7/1.15.

**Contaminants:** None detected.

**Form:** Supplied in 20mM Tris, 150mM NaCl, 5mM CaCl<sub>2</sub>, pH 7.5.

**Biohazard:** Blood sample from tissue donors tested negative for HBsAg, HIV-1 and HIV-2 antibodies, HCV and Syphilis.

**Storage:** Ships on DRY ICE. Upon receipt store at -70°C. Avoid multiple freeze thaw cycles

**Additional Remarks:**

Unless otherwise noted on this datasheet, the requalification/expiration date for all products is 2 years from the date of receipt to the customer

**FOR INVITRO USE ONLY**

CAUTION: Not for use in humans or clinical diagnosis: This product is intended for research or manufacturing use only. It is pharmaceutically unrefined, and verification of its suitability for use in humans or as clinical diagnostic reagents and the compliance with all Federal and State laws regulating such applications are the responsibility of the purchaser. There is no expressed or implied warranty. No liability is assumed for fitness or purpose and merchantability, or direct or consequential damages. The user names assumes all responsibility for care, custody and control of the material, including its disposal, in accordance with all regulations.

FM 4.15-5

Fitzgerald Industries International is registered under the company name Benen Trading Limited.

**Appendix B. Experimental details of the Qualitative LC-MS analysis of SRM 2921a**

**Method Name** IntactTroponin\_29Mar24.m  
**Method Path** D:\MassHunter\Methods\David\IntactTroponin\_29Mar24.m  
**Method Description** LC-TOF method for analysis of human troponin complex

**TOF/Q-TOF Mass Spectrometer**

Component Name	MS Q-TOF	Component Model	G6550A
Ion Source	Dual AJS ESI	Stop Time (min)	45.00
MS Abs. threshold	1	MS Rel. threshold(%)	0.000
MS/MS Abs. threshold	5	MS/MS Rel. threshold(%)	0.010

Min Range (m/z)	650
Max Range (m/z)	1650
Scan Rate (spectra/sec)	2.00

Gas Temp (°C)	250
Gas Flow (l/min)	14
Nebulizer (psig)	20
SheathGasTemp	350
SheathGasFlow	12

VCap	4500
Nozzle Voltage (V)	2000
Fragmentor	300
Skimmer1	65
OctopoleRFPeak	750

<b>Low Flow HiP Sampler</b>	<b>Model:</b>	<b>G1377A</b>
-----------------------------	---------------	---------------

Draw Speed	10.0 µL/min
Eject Speed	10.0 µL/min
Draw Position Offset	1.5 mm
Wait Time After Drawing	2.0 s
Sample Flush Out Factor	1.5
Vial/Well bottom sensing	Yes

Injection Mode	Injection with needle wash
----------------	----------------------------

Injection Volume	5.00 $\mu\text{L}$
------------------	--------------------

Needle Wash Location	Flush Port
Wash Time	5.0 s

<b>Cap Pump</b>	<b>Model:</b>	<b>G1376A</b>
-----------------	---------------	---------------

Flow	15.00 $\mu\text{L}/\text{min}$
Low Pressure Limit	0.00 bar
High Pressure Limit	300.00 bar
Maximum Flow Gradient	100.000 $\text{mL}/\text{min}^2$
Operation Mode	Micro Flow

Compressibility Mode A	Compressibility Value Set
Compressibility A	50 10e-6/bar

**Mobile Phase A** = 0.5 % (v/v) formic acid in water

**Mobile Phase B** = 0.5 % (v/v) formic acid in acetonitrile

	Time	A	B	Flow	Pressure
1	5.00 min	75.0 %	25.0 %	15.00 $\mu\text{L}/\text{min}$	300.00 bar
2	20.00 min	20.0 %	80.0 %	15.00 $\mu\text{L}/\text{min}$	300.00 bar
3	25.00 min	0.0 %	100.0 %	15.00 $\mu\text{L}/\text{min}$	300.00 bar
4	30.00 min	75.0 %	25.0 %	15.00 $\mu\text{L}/\text{min}$	300.00 bar
5	45.00 min	75.0 %	25.0 %	15.00 $\mu\text{L}/\text{min}$	300.00 bar

<b>Column Comp.</b>	<b>Model:</b>	<b>G1316A</b>
---------------------	---------------	---------------

Temperature Control Mode	Temperature Set
Temperature	50.0 $^{\circ}\text{C}$

**Column** = Agilent Zorbax 300SB-C18 (0.5 mm x 150 mm; 3.5 micron)

### Appendix C. Agilent LC-MS SIM Method Parameters

Method Name IntactTroponin\_SIM\_01Mar24.m  
 Method Path D:\MassHunter\Data\David\Methods\IntactTroponin\_SIM\_01Mar24.m  
 Method Description SIM method for three charge state ions of cTnI using mobile phases with 0.1 % TFA

#### MS QQQ Mass Spectrometer Model:

Ion Source	AJS ESI
Stop Mode	By StopTime
Time Filter	On

Tune File	D:\MassHunter\Tune\QQQ\G6460A\atunes.tune.xml
Stop Time (min)	20
Time Filter Width (min)	0.1

Start Time (min)	Scan Type	Ion Mode	Div Valve	Delta EMV (+)	Store
0	MS2 Scan	ESI+Agilent Jet Stream	To Waste	100	No
5	MS2 SIM	ESI+Agilent Jet Stream	To MS	100	Yes

Start Mass	End Mass	Scan Time	Frag (V)	Cell Acc (V)	Polarity
750	1500	250	100	5	Positive

Gas Temp (°C)	300
Gas Flow (l/min)	10
Nebulizer (psi)	40

Sheath Gas Temp (°C)	300
Sheath Gas Flow (l/min)	8
Capillary (V)	3500
Nozzle Voltage/Charging (V)	500

Cpd Group	Cpd Name	ISTD?	Mass	MS2 Res	Dwell	Frag (V)	Cell Acc (V)	Polarity
cTnl	27+ peak	No	886.8	Unit/Enh (6490)	125	150	7	Positive
cTnl	28+ peak	No	855.1	Unit/Enh (6490)	125	150	7	Positive
cTnl	29+ peak	No	825.7	Unit/Enh (6490)	125	150	7	Positive

<b>HiP Sampler</b>	<b>Model: G4226A</b>
Draw Speed	50.0 µL/min
Eject Speed	10.0 µL/min
Draw Position Offset	2.0 mm
Wait Time After Drawing	5.0 s
Sample Flush Out Factor	7.5
Vial/Well bottom sensing	Yes
Injection Mode	Injection with needle wash
Injection Volume	5.00 µL
Needle Wash Location	Flush Port
Wash Time	5.0 s

<b>Binary Pump</b>	<b>Model: G4220A</b>
Flow	0.250 mL/min
Use Solvent Types	Yes
Stroke Mode	Synchronized
Low Pressure Limit	0.00 bar
High Pressure Limit	200.00 bar
Max. Flow Ramp Up	100.000 mL/min <sup>2</sup>
Max. Flow Ramp Down	100.000 mL/min <sup>2</sup>
Expected Mixer	Jet Weaver V35 Mixer

Mobile Phase A = 0.1 % (v/v) trifluoroacetic acid in water

Mobile Phase B = 0.1 % (v/v) trifluoroacetic acid in acetonitrile

<b>Time</b>	<b>A</b>	<b>B</b>	<b>Flow</b>
5.00 min	70.00 %	30.00 %	0.250 mL/min
20.00 min	10.00 %	90.00 %	0.250 mL/min
25.00 min	0.00 %	100.00 %	0.250 mL/min
30.00 min	70.00 %	30.00 %	0.250 mL/min
45.00 min	70.00 %	30.00 %	0.250 mL/min

<b>Column Comp.</b>	<b>Model: G1316C</b>
Temperature Control Mode	Temperature Set
Temperature	45.0 °C

Column = Agilent Zorbax 300SB-C8 column (2.1 mm x 150 mm, 5 µm particle size)

## Appendix D. Agilent LC-MS Needle and Column Wash Method Parameters

<b>Method Name</b>	Needle+ColumnWash_27Feb24.m
<b>Method Path</b>	D:\MassHunter\Data\David\Methods\Needle+ColumnWash_27Feb24.m
<b>Method Description</b>	Column and Needle Wash method for sticky intact protein LC-MS

### Name: HiP Sampler

Module: G4226A

Auxiliary	
Draw Speed	50.0 µL/min
Eject Speed	10.0 µL/min
Draw Position Offset	2.0 mm
Wait Time After Drawing	2.0 s
Sample Flush Out Factor	7.5
Vial/Well bottom sensing	Yes
Injection	
Injection Mode	Injection with needle wash
Injection Volume	10.00 µL
Needle Wash	
Needle Wash Location	Wash Vial
Wash Location	P1-A-9
Wash Cycles	5
High throughput	
Automatic Delay Volume Reduction	No
Overlapped Injection	
Enable Overlapped Injection	No
Valve Switching	
Valve Movements	1
Valve Switch Time 1	
Switch Time 1 Enabled	Yes
Switch Time 1	0.50 min
Valve Switch Time 2	
Switch Time 2 Enabled	Yes
Switch Time 2	5.00 min
Valve Switch Time 3	
Switch Time 3 Enabled	Yes
Switch Time 3	5.50 min
Valve Switch Time 4	
Switch Time 4 Enabled	Yes
Switch Time 4	35.00 min

### Name: Binary Pump

Module: G4220A

Flow	0.250 mL/min
Use Solvent Types	Yes
Stroke Mode	Synchronized
Low Pressure Limit	0.00 bar
High Pressure Limit	200.00 bar

**Max. Flow Ramp Up**  
**Max. Flow Ramp Down**  
**Expected Mixer**

100.000 mL/min<sup>2</sup>  
100.000 mL/min<sup>2</sup>  
Jet Weaver V35 Mixer

Mobile Phase A = 0.1 % (v/v) trifluoroacetic acid in water

Mobile Phase B = 0.1 % (v/v) trifluoroacetic acid in acetonitrile

<b>Time (min)</b>	<b>A (%)</b>	<b>B (%)</b>	<b>Flow (mL/min)</b>
5.00 min	0.00 %	100.00 %	0.250 mL/min
15.00 min	30.00 %	70.00 %	0.250 mL/min
20.00 min	90.00 %	10.00 %	0.250 mL/min
25.00 min	20.00 %	80.00 %	0.250 mL/min
30.00 min	70.00 %	30.00 %	0.250 mL/min
45.00 min	70.00 %	30.00 %	0.250 mL/min

**Name: Column Comp.**

**Module: G1316C**

Temperature Control Mode  
Temperature

Temperature Set  
45.0 °C

**Appendix E. Typical worklist for the acquisition of certification data from a measurement set**

Sample Name	Sample Position	Method	Data File	Comment
Column+ Needle Wash	P1-A1	Needle+ColumnWash_27Feb 24.m	Wash_03Apr24_01.d	
Blank	P1-A1	IntactTroponin_SIM_01Mar2 4.m	Blank_03Apr24_01.d	0.1 % TFA in water
Column+ Needle Wash	P1-A1	Needle+ColumnWash_27Feb 24.m	Wash_03Apr24_02.d	
Cal 1-1	P1-B1	IntactTroponin_SIM_01Mar2 4.m	Cal 1-1_03Apr24_01.d	Cal 1-1 prepared 03Apr24
Column+ Needle Wash	P1-A1	Needle+ColumnWash_27Feb 24.m	Wash_03Apr24_03.d	
Cal 1-1	P1-B1	IntactTroponin_SIM_01Mar2 4.m	Cal 1-1_03Apr24_02.d	Cal 1-1 prepared 03Apr24
Column+ Needle Wash	P1-A1	Needle+ColumnWash_27Feb 24.m	Wash_03Apr24_04.d	
Cal 1-1	P1-B1	IntactTroponin_SIM_01Mar2 4.m	Cal 1-1_03Apr24_03.d	Cal 1-1 prepared 03Apr24
Column+ Needle Wash	P1-A1	Needle+ColumnWash_27Feb 24.m	Wash_03Apr24_05.d	
Cal 1-1	P1-B1	IntactTroponin_SIM_01Mar2 4.m	Cal 1-1_03Apr24_04.d	Cal 1-1 prepared 03Apr24
Column+ Needle Wash	P1-A1	Needle+ColumnWash_27Feb 24.m	Wash_03Apr24_06.d	
Blank	P1-A1	IntactTroponin_SIM_01Mar2 4.m	Blank_03Apr24_02.d	0.1 % TFA in water
Column+ Needle Wash	P1-A1	Needle+ColumnWash_27Feb 24.m	Wash_03Apr24_07.d	
SRM2921a-2	P1-D1	IntactTroponin_SIM_01Mar2 4.m	SRM2921a_Box2_03Apr24_ 01.d	SRM 2921a from Box 2
Column+ Needle Wash	P1-A1	Needle+ColumnWash_27Feb 24.m	Wash_03Apr24_08.d	
SRM2921a-2	P1-D1	IntactTroponin_SIM_01Mar2 4.m	SRM2921a_Box2_03Apr24_ 02.d	SRM 2921a from Box 2
Column+ Needle Wash	P1-A1	Needle+ColumnWash_27Feb 24.m	Wash_03Apr24_09.d	
SRM2921a-2	P1-D1	IntactTroponin_SIM_01Mar2 4.m	SRM2921a_Box2_03Apr24_ 03.d	SRM 2921a from Box 2
Column+ Needle Wash	P1-A1	Needle+ColumnWash_27Feb 24.m	Wash_03Apr24_10.d	
Blank	P1-A1	IntactTroponin_SIM_01Mar2 4.m	Blank_03Apr24_03.d	0.1 % TFA in water
Column+ Needle Wash	P1-A1	Needle+ColumnWash_27Feb 24.m	Wash_03Apr24_11.d	
SRM2921a-8	P1-D2	IntactTroponin_SIM_01Mar2 4.m	SRM2921a_Box8_03Apr24_ 01.d	SRM 2921a from Box 8
Column+ Needle Wash	P1-A1	Needle+ColumnWash_27Feb 24.m	Wash_03Apr24_12.d	
SRM2921a-8	P1-D2	IntactTroponin_SIM_01Mar2 4.m	SRM2921a_Box8_03Apr24_ 02.d	SRM 2921a from Box 8
Column+ Needle Wash	P1-A1	Needle+ColumnWash_27Feb 24.m	Wash_03Apr24_13.d	

SRM2921a-8	P1-D2	IntactTroponin_SIM_01Mar24.m	SRM2921a_Box8_03Apr24_03.d	SRM 2921a from Box 8
Column+ Needle Wash	P1-A1	Needle+ColumnWash_27Feb24.m	Wash_03Apr24_14.d	
Blank	P1-A1	IntactTroponin_SIM_01Mar24.m	Blank_03Apr24_04.d	0.1 % TFA in water
Column+ Needle Wash	P1-A1	Needle+ColumnWash_27Feb24.m	Wash_03Apr24_15.d	
Cal 2-1	P1-B2	IntactTroponin_SIM_01Mar24.m	Cal 2-1_03Apr24_01.d	Cal 2-1 prepared 03Apr24
Column+ Needle Wash	P1-A1	Needle+ColumnWash_27Feb24.m	Wash_03Apr24_16.d	
Cal 2-1	P1-B2	IntactTroponin_SIM_01Mar24.m	Cal 2-1_03Apr24_02.d	Cal 2-1 prepared 03Apr24
Column+ Needle Wash	P1-A1	Needle+ColumnWash_27Feb24.m	Wash_03Apr24_17.d	
Cal 2-1	P1-B2	IntactTroponin_SIM_01Mar24.m	Cal 2-1_03Apr24_03.d	Cal 2-1 prepared 03Apr24
Column+ Needle Wash	P1-A1	Needle+ColumnWash_27Feb24.m	Wash_03Apr24_18.d	
Blank	P1-A1	IntactTroponin_SIM_01Mar24.m	Blank_03Apr24_05.d	0.1 % TFA in water
Column+ Needle Wash	P1-A1	Needle+ColumnWash_27Feb24.m	Wash_03Apr24_19.d	
Cal 1-2	P1-C1	IntactTroponin_SIM_01Mar24.m	Cal 1-2_03Apr24_01.d	Cal 1-2 prepared 03Apr24
Column+ Needle Wash	P1-A1	Needle+ColumnWash_27Feb24.m	Wash_03Apr24_20.d	
Cal 1-2	P1-C1	IntactTroponin_SIM_01Mar24.m	Cal 1-2_03Apr24_02.d	Cal 1-2 prepared 03Apr24
Column+ Needle Wash	P1-A1	Needle+ColumnWash_27Feb24.m	Wash_03Apr24_21.d	
Cal 1-2	P1-C1	IntactTroponin_SIM_01Mar24.m	Cal 1-2_03Apr24_03.d	Cal 1-2 prepared 03Apr24
Column+ Needle Wash	P1-A1	Needle+ColumnWash_27Feb24.m	Wash_03Apr24_22.d	
Blank	P1-A1	IntactTroponin_SIM_01Mar24.m	Blank_03Apr24_06.d	0.1 % TFA in water
Column+ Needle Wash	P1-A1	Needle+ColumnWash_27Feb24.m	Wash_03Apr24_23.d	
SRM2921a-9	P1-D3	IntactTroponin_SIM_01Mar24.m	SRM2921a_Box9_03Apr24_01.d	SRM 2921a from Box 9
Column+ Needle Wash	P1-A1	Needle+ColumnWash_27Feb24.m	Wash_03Apr24_24.d	
SRM2921a-9	P1-D3	IntactTroponin_SIM_01Mar24.m	SRM2921a_Box9_03Apr24_02.d	SRM 2921a from Box 9
Column+ Needle Wash	P1-A1	Needle+ColumnWash_27Feb24.m	Wash_03Apr24_25.d	
SRM2921a-9	P1-D3	IntactTroponin_SIM_01Mar24.m	SRM2921a_Box9_03Apr24_03.d	SRM 2921a from Box 9
Column+ Needle Wash	P1-A1	Needle+ColumnWash_27Feb24.m	Wash_03Apr24_26.d	
Blank	P1-A1	IntactTroponin_SIM_01Mar24.m	Blank_03Apr24_07.d	0.1 % TFA in water

Column+ Needle Wash	P1-A1	Needle+ColumnWash_27Feb 24.m	Wash_03Apr24_27.d	
SRM2921a-13	P1-D4	IntactTroponin_SIM_01Mar2 4.m	SRM2921a_Box13_03Apr24 01.d	SRM 2921a from Box 13
Column+ Needle Wash	P1-A1	Needle+ColumnWash_27Feb 24.m	Wash_03Apr24_28.d	
SRM2921a-13	P1-D4	IntactTroponin_SIM_01Mar2 4.m	SRM2921a_Box13_03Apr24 02.d	SRM 2921a from Box 13
Column+ Needle Wash	P1-A1	Needle+ColumnWash_27Feb 24.m	Wash_03Apr24_29.d	
SRM2921a-13	P1-D4	IntactTroponin_SIM_01Mar2 4.m	SRM2921a_Box13_03Apr24 03.d	SRM 2921a from Box 13
Column+ Needle Wash	P1-A1	Needle+ColumnWash_27Feb 24.m	Wash_03Apr24_30.d	
Blank	P1-A1	IntactTroponin_SIM_01Mar2 4.m	Blank_03Apr24_08.d	0.1 % TFA in water
Column+ Needle Wash	P1-A1	Needle+ColumnWash_27Feb 24.m	Wash_03Apr24_31.d	
Cal 2-2	P1-C2	IntactTroponin_SIM_01Mar2 4.m	Cal 2-2_03Apr24_01.d	Cal 2-2 prepared 03Apr24
Column+ Needle Wash	P1-A1	Needle+ColumnWash_27Feb 24.m	Wash_03Apr24_32.d	
Cal 2-2	P1-C2	IntactTroponin_SIM_01Mar2 4.m	Cal 2-2_03Apr24_02.d	Cal 2-2 prepared 03Apr24
Column+ Needle Wash	P1-A1	Needle+ColumnWash_27Feb 24.m	Wash_03Apr24_33.d	
Cal 2-2	P1-C2	IntactTroponin_SIM_01Mar2 4.m	Cal 2-2_03Apr24_03.d	Cal 2-2 prepared 03Apr24
Column+ Needle Wash	P1-A1	Needle+ColumnWash_27Feb 24.m	Wash_03Apr24_34.d	
Blank	P1-A1	IntactTroponin_SIM_01Mar2 4.m	Blank_03Apr24_09.d	0.1 % TFA in water

**Appendix F. Certification data from the LC-MS analysis of SRM 2921a using SIMS. The Box number refers to the storage box (containing 100 vials) from which the sample of SRM 2921a was removed**

Set	Box	Technical Replicate	[cTnl], mg/L
1	1	1	135.14
1	1	2	135.60
1	1	3	134.50
1	5	1	133.94
1	5	2	136.78
1	5	3	136.00
1	29	1	130.81
1	29	2	131.40
1	29	3	127.90
1	26	1	129.88
1	26	2	130.93
1	26	3	129.87
2	3	1	144.68
2	3	2	142.91
2	3	3	146.01
2	17	1	135.95
2	17	2	141.63
2	17	3	139.92
2	24	1	138.16
2	24	2	138.61
2	24	3	141.21
2	25	1	137.20
2	25	2	137.61
2	25	3	137.72
3	8	1	134.74
3	8	2	130.84
3	8	3	130.24
3	13	1	135.49
3	13	2	134.68
3	13	3	132.34
3	19	1	134.94
3	19	2	134.60
3	19	3	132.37
3	20	1	137.62
3	20	2	135.96
3	20	3	134.35
4	2	1	149.38
4	2	2	143.55

4	2	3	140.08
4	7	1	151.89
4	7	2	145.00
4	7	3	137.82
4	9	1	148.26
4	9	2	139.14
4	9	3	131.03
4	12	1	148.41
4	12	2	142.61
4	12	3	139.17
5	2	1	153.36
5	2	2	147.08
5	2	3	139.07
5	8	1	151.78
5	8	2	147.67
5	8	3	146.39
5	9	1	153.31
5	9	2	151.34
5	9	3	149.05
5	13	1	152.25
5	13	2	152.40
5	13	3	149.01

**Appendix G. Gravimetric sample and calibration solutions preparation data and raw analysis data from certification sets**

**Set 1:**

**SRM 2921A Certification Set 1**

Date = 12-Mar-24

<b>Sample</b>	<b>Volume 2921,</b> μL	<b>Weight 2921,</b> g	<b>Volume Diluent,</b> μL	<b>Weight Diluent,</b> g	<b>Dilution Factor</b>
Cal 1-1	78	0.07583	42	0.04420	0.632
Cal 2-1	100	0.09688	0	0	1.000
Cal 1-2	78	0.07851	42	0.04468	0.637
Cal 2-2	100	0.09952	0	0	1.000

Diluent = 0.1 % TFA in LC-MS grade water Samples/Calibrants weighed into Eppendorf 0.5 mL Protein LoBind tubes

<b>Sample</b>	<b>Volume 2921A,</b> μL	<b>Weight 2921A,</b> g	<b>Volume Diluent,</b> μL	<b>Weight Diluent,</b> g	<b>Dilution Factor</b>
2921A-1	78	0.07682	322	0.32332	0.192
2921A-5	78	0.07887	322	0.32273	0.196
2921A-29	78	0.07733	322	0.32330	0.193
2921A-26	78	0.07611	322	0.32308	0.191

Balance = Mettler XP205 (227/B143, NIST #N107272)

Temperature = 69 °F

Relative Humidity = 37%

Analysis Dates = 12-Mar-24 to 14-Mar-24

Mobile Phase = 0.1 % TFA in LC-MS grade H2O and Acetonitrile

TFA = EMB Millipore, product # TX1275-1, lot # 55344627

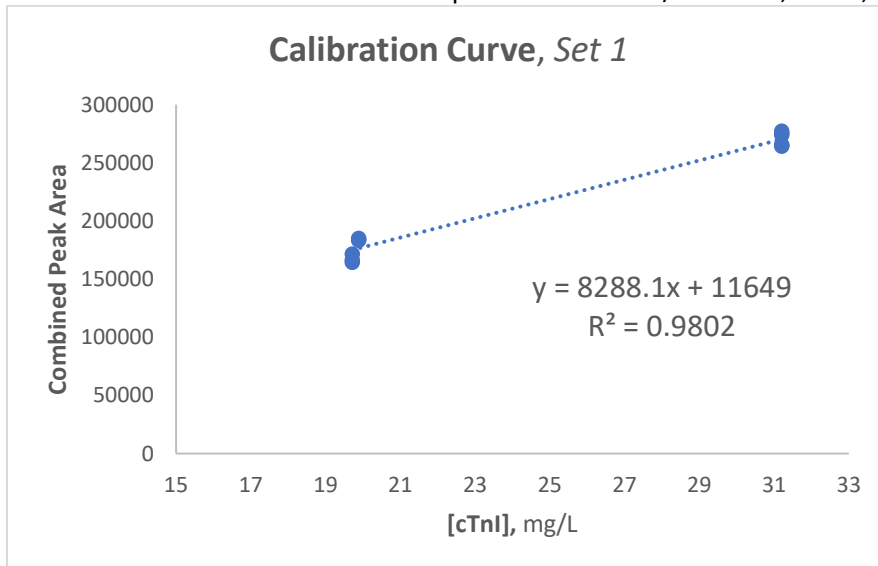
Column = Agilent Zorbax 300SB-C8 (2.1 x 150 mm, 5 μm, part # 883750-906, lot # USHC001483)

<b>Sample</b>	<b>Combined Peak Area*</b>	<b>[cTnl], mg/L</b>
Cal 1-1-2	171606	19.71
Cal 1-1-3	164480	19.71
Cal 1-1-4	166474	19.71
Cal 2-1-1	277195	31.20
Cal 2-1-2	273839	31.20
Cal 2-1-3	275239	31.20
Cal 1-2-1	185024	19.88

Cal 1-2-2	183322	19.88
Cal 1-2-3	183834	19.88
Cal 2-2-1	265069	31.20
Cal 2-2-2	265326	31.20
Cal 2-2-3	264416	31.20

		Sample [cTnI], mg/L	2921a [cTnI], mg/L
2921a-1-1	226684	25.95	135.14
2921a-1-2	227414	26.03	135.60
2921a-1-3	225663	25.82	134.50
2921a-5-1	229658	26.30	133.94
2921a-5-2	234292	26.86	136.78
2921a-5-3	233019	26.71	136.00
2921a-29-1	220920	25.25	130.81
2921a-29-2	221863	25.36	131.40
2921a-29-3	216253	24.69	127.90
2921a-26-1	216884	24.76	129.88
2921a-26-2	218539	24.96	130.93
2921a-26-3	216867	24.76	129.87

\* = combined SIM peak area from m/z = 825.7, 855.1, and 886.8



**Set 2:**

**SRM 2921A Certification Set 2**

Date = 15-Mar-24

Sample	Volume 2921, μL	Weight 2921, g	Volume Diluent, μL	Weight Diluent, g	Dilution Factor
--------	--------------------	----------------	--------------------	----------------------	--------------------

Cal 1-1	78	0.07704	42	0.04392	0.637
Cal 2-1	100	0.09949	0	0	1.000
Cal 1-2	78	0.07932	42	0.04392	0.644
Cal 2-2	100	0.10275	0	0	1.000

Diluent = 0.1 % TFA in LC-MS grade water      Samples/Calibrants weighed into Eppendorf 0.5 mL Protein LoBind tubes

Sample	Volume 2921A, $\mu\text{L}$	Weight 2921A, g	Volume Diluent, $\mu\text{L}$	Weight Diluent, g	Dilution Factor
2921A-3	78	0.07918	322	0.32261	0.197
2921A-17	78	0.07728	322	0.32169	0.194
2921A-24	78	0.08090	322	0.32220	0.201
2921A-25	78	0.07663	322	0.32188	0.192

Balance = Mettler XP205 (227/B143, NIST #N107272)  
Temperature = 72 °F  
Relative Humidity = 55%

Analysis Dates = 15-Mar-24 to 17-Mar-24

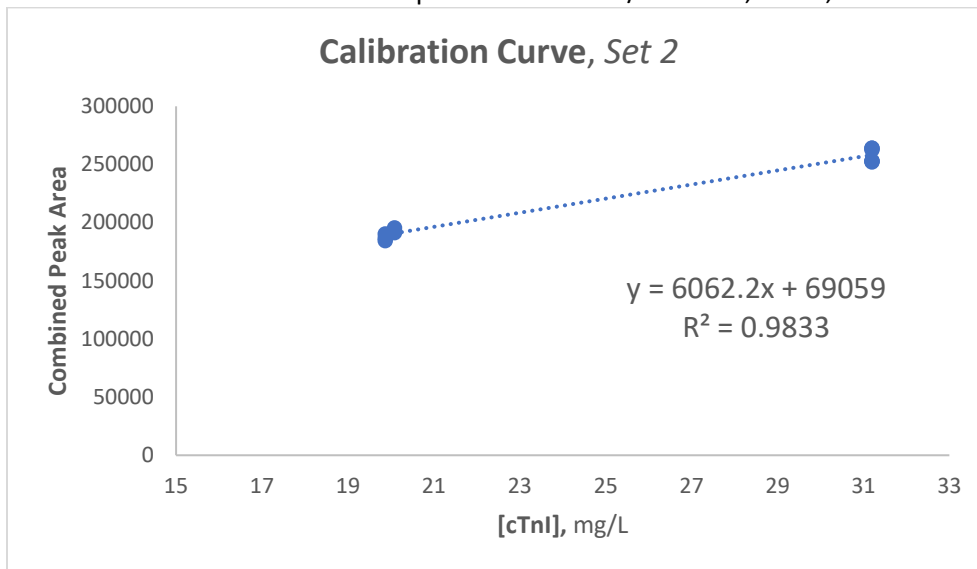
Mobile Phase = 0.1 % TFA in LC-MS grade H2O and Acetonitrile  
TFA = EMB Millipore, product # TX1275-1, lot # 55344627  
Column = Agilent Zorbax 300SB-C8 (2.1 x 150 mm, 5  $\mu\text{m}$ , part # 883750-906, lot # USHC001483)

Sample	Combined Peak Area*	[cTnl], mg/L
Cal 1-1-2	190251	19.87
Cal 1-1-3	186762	19.87
Cal 1-1-4	184596	19.87
Cal 2-1-1	252908	31.20
Cal 2-1-2	253043	31.20
Cal 2-1-3	252286	31.20
Cal 1-2-1	192644	20.08
Cal 1-2-2	195415	20.08
Cal 1-2-3	191417	20.08
Cal 2-2-1	262726	31.20
Cal 2-2-2	264041	31.20
Cal 2-2-3	264064	31.20

		Sample [cTnl], mg/L	2921a [cTnl], mg/L
2921a-3-1	241909	28.51	144.68
2921a-3-2	239783	28.16	142.91
2921a-3-3	243487	28.77	146.01

2921a-17-1	228694	26.33	135.95
2921a-17-2	235363	27.43	141.63
2921a-17-3	233353	27.10	139.92
2921a-24-1	237157	27.73	138.16
2921a-24-2	237698	27.82	138.61
2921a-24-3	240861	28.34	141.21
2921a-25-1	228999	26.38	137.20
2921a-25-2	229473	26.46	137.61
2921a-25-3	229598	26.48	137.72

\* = combined SIM peak area from m/z = 825.7, 855.1, and 886.8



**Set 3:**

**SRM 2921A Certification Set 3**

Date = 18-Mar-24

Sample	Volume 2921, μL	Weight 2921, g	Volume Diluent, μL	Weight Diluent, g	Dilution Factor
Cal 1-1	78	0.07889	42	0.04383	0.643
Cal 2-1	100	0.10104	0	0	1.000
Cal 1-2	78	0.07946	42	0.04332	0.647
Cal 2-2	100	0.0996	0	0	1.000

Diluent = 0.1 % TFA in LC-MS grade water

Samples/Calibrants weighed into Eppendorf 0.5 mL Protein LoBind tubes

Sample	Volume 2921A, μL	Weight 2921A, g	Volume Diluent, μL	Weight Diluent, g	Dilution Factor
--------	---------------------	--------------------	-----------------------	----------------------	--------------------

2921A-8	78	0.07981	322	0.32199	0.199
2921A-13	78	0.07983	322	0.32195	0.199
2921A-19	78	0.07864	322	0.32122	0.197
2921A-20	78	0.07869	322	0.32163	0.197

Balance = Mettler XP205 (227/B143, NIST #N107272)  
 Temperature = 70 °F  
 Relative Humidity = 36%

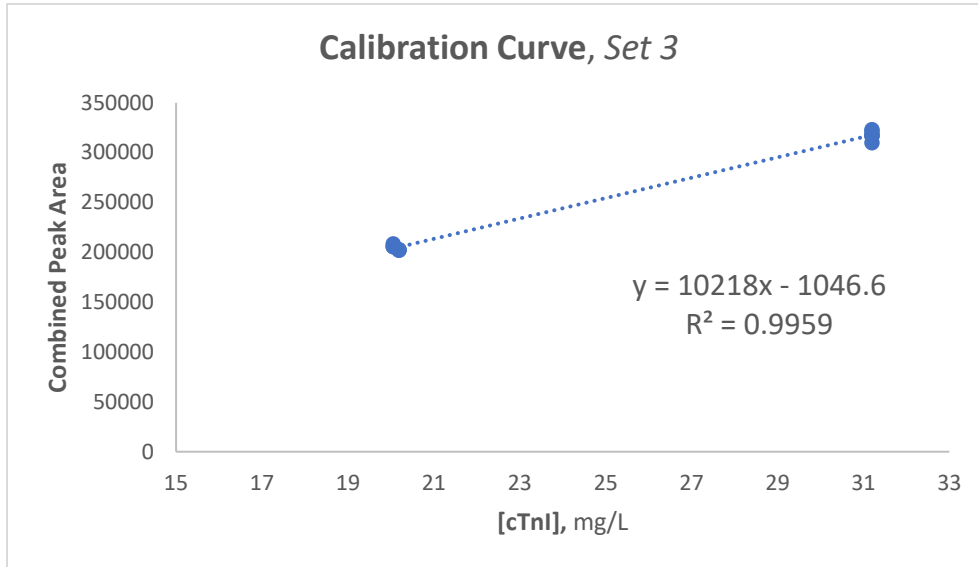
Analysis Dates  
 = 19-Mar-24 to 21-Mar-24

Mobile Phase = 0.1 % TFA in LC-MS grade H2O and Acetonitrile  
 TFA = EMB Millipore, product # TX1275-1, lot # 55344627  
 Column = Agilent Zorbax 300SB-C8 (2.1 x 150 mm, 5 µm, part # 883750-906, lot # USHC001483)

Sample	Combined Peak Area*	[cTnl], mg/L
Cal 1-1-2	205898	20.06
Cal 1-1-3	205677	20.06
Cal 1-1-4	208489	20.06
Cal 2-1-1	309924	31.20
Cal 2-1-2	317081	31.20
Cal 2-1-3	316636	31.20
Cal 1-2-1	202821	20.19
Cal 1-2-2	202367	20.19
Cal 1-2-3	202206	20.19
Cal 2-2-1	321595	31.20
Cal 2-2-2	318311	31.20
Cal 2-2-3	323179	31.20

		Sample [cTnl], mg/L	2921a [cTnl], mg/L
2921a-8-1	274523	26.76	134.74
2921a-8-2	266599	25.99	130.84
2921a-8-3	265387	25.87	130.24
2921a-13-1	276126	26.92	135.49
2921a-13-2	274486	26.76	134.68
2921a-13-3	269727	26.29	132.34
2921a-19-1	272213	26.54	134.94
2921a-19-2	271544	26.47	134.60
2921a-19-3	267062	26.03	132.37
2921a-20-1	277470	27.05	137.62
2921a-20-2	274133	26.73	135.96
2921a-20-3	270883	26.41	134.35

\* = combined SIM peak area from m/z = 825.7, 855.1, and 886.8



**Set 4:**

**SRM 2921A Certification Set 4**

Date = 26-Mar-24

Sample	Volume 2921, μL	Weight 2921, g	Volume Diluent, μL	Weight Diluent, g	Dilution Factor
Cal 1-1	78	0.07809	42	0.04405	0.639
Cal 2-1	100	0.09688	0	0	1.000
Cal 1-2	78	0.07829	42	0.04369	0.642
Cal 2-2	100	0.10107	0	0	1.000

Diluent = 0.1 % TFA in LC-MS grade water

Samples/Calibrants weighed into Eppendorf 0.5 mL Protein LoBind tubes

Sample	Volume 2921A, μL	Weight 2921A, g	Volume Diluent, μL	Weight Diluent, g	Dilution Factor
2921A-2	78	0.07978	322	0.32119	0.199
2921A-7	78	0.08049	322	0.32238	0.200
2921A-9	78	0.07874	322	0.32231	0.196
2921A-12	78	0.08031	322	0.32069	0.200

Balance = Mettler XP205 (227/B143, NIST #N107272)

Temperature = 72 °F

Relative Humidity = 36%

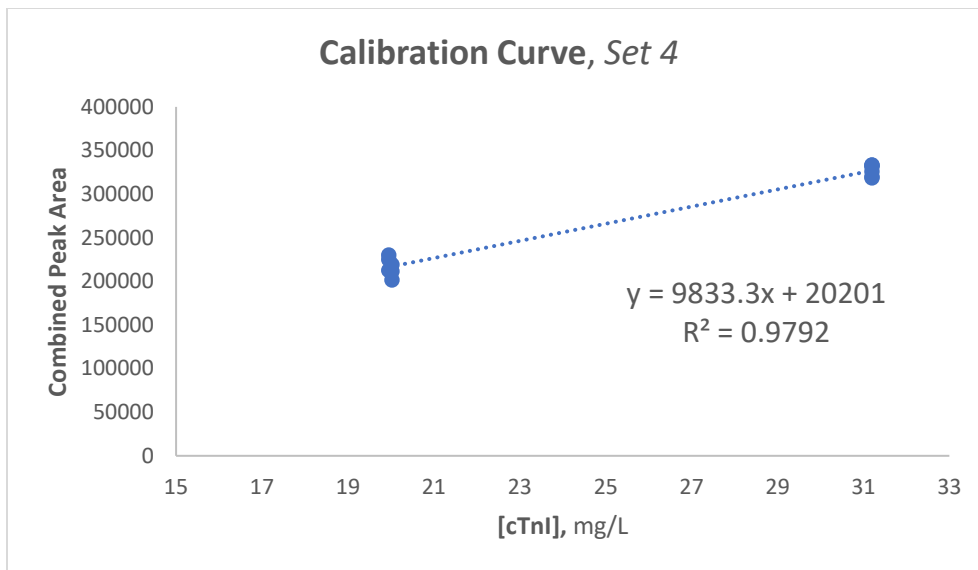
Analysis Dates = 26-Mar-24 to 28-Mar-24

Mobile Phase = 0.1 % TFA in LC-MS grade H2O and Acetonitrile  
TFA = EMB Millipore, product # TX1275-1, lot # 55344627  
Column = Agilent Zorbax 300SB-C8 (2.1 x 150 mm, 5 µm, part # 883750-906, lot # USHC001483)

Sample	Combined Peak Area*	[cTnl], mg/L
Cal 1-1-2	230262	19.95
Cal 1-1-3	225056	19.95
Cal 1-1-4	212663	19.95
Cal 2-1-1	333022	31.20
Cal 2-1-2	331329	31.20
Cal 2-1-3	333335	31.20
Cal 1-2-1	219234	20.02
Cal 1-2-2	211475	20.02
Cal 1-2-3	201569	20.02
Cal 2-2-1	325740	31.20
Cal 2-2-2	318660	31.20
Cal 2-2-3	320038	31.20

		Sample [cTnl], mg/L	2921a [cTnl], mg/L
2921a-2-1	312465	29.72	149.38
2921a-2-2	301050	28.56	143.55
2921a-2-3	294273	27.87	140.08
2921a-7-1	318615	30.35	151.89
2921a-7-2	305071	28.97	145.00
2921a-7-3	290961	27.54	137.82
2921a-9-1	306436	29.11	148.26
2921a-9-2	288830	27.32	139.14
2921a-9-3	273167	25.73	131.03
2921a-12-1	312465	29.72	148.41
2921a-12-2	301050	28.56	142.61
2921a-12-3	294273	27.87	139.17

\* = combined SIM peak area from m/z = 825.7, 855.1, and 886.8



**Set 5:**

**SRM 2921A Certification Set 5**

Date = 3-Apr-24

Sample	Volume 2921, μL	Weight 2921, g	Volume Diluent, μL	Weight Diluent, g	Dilution Factor
Cal 1-1	78	0.07910	42	0.04405	0.642
Cal 2-1	100	0.10176	0	0	1.000
Cal 1-2	78	0.07650	42	0.04393	0.635
Cal 2-2	100	0.10156	0	0	1.000

Diluent = 0.1 % TFA in LC-MS grade water

Samples/Calibrants weighed into Eppendorf 0.5 mL Protein LoBind tubes

Sample	Volume 2921A, μL	Weight 2921A, g	Volume Diluent, μL	Weight Diluent, g	Dilution Factor
2921A-2	78	0.07929	322	0.32187	0.198
2921A-8	78	0.08052	322	0.32194	0.200
2921A-9	78	0.08104	322	0.32173	0.201
2921A-13	78	0.08058	322	0.32129	0.201

Balance = Mettler XP205 (227/B143, NIST #N107272)

Temperature = 73 °F

Relative Humidity = 50%

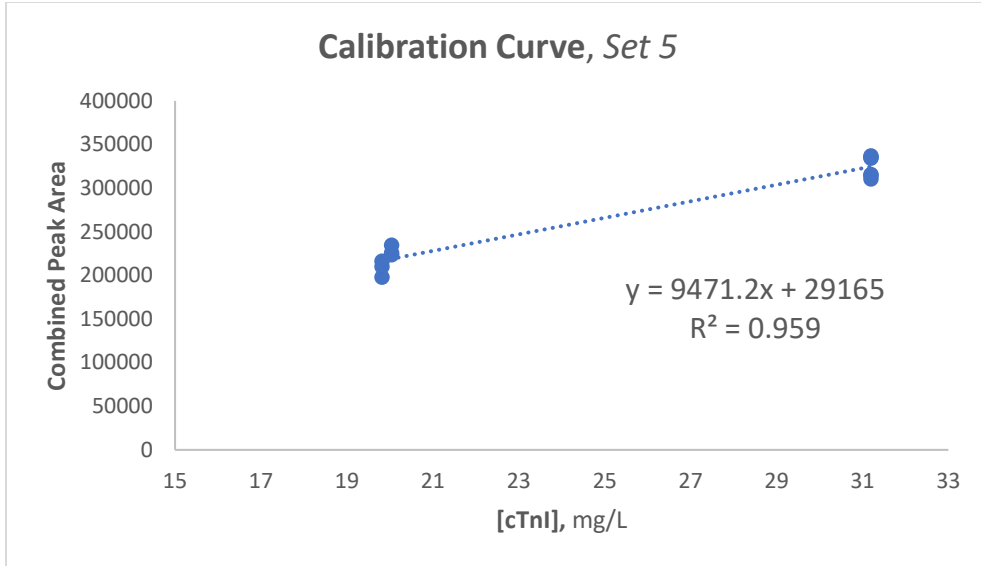
Analysis Dates = 3-Apr-24 to 5-Apr-24

Mobile Phase = 0.1 % TFA in LC-MS grade H2O and Acetonitrile  
 TFA = EMB Millipore, product # TX1275-1, lot # 55344627  
 Column = Agilent Zorbax 300SB-C8 (2.1 x 150 mm, 5 µm, part # 883750-906, lot # USHC001483)

Sample	Combined Peak Area*	[cTnl], mg/L
Cal 1-1-2	234447	20.04
Cal 1-1-3	225805	20.04
Cal 1-1-4	223624	20.04
Cal 2-1-1	315703	31.20
Cal 2-1-2	314477	31.20
Cal 2-1-3	310494	31.20
Cal 1-2-1	216223	19.82
Cal 1-2-2	209974	19.82
Cal 1-2-3	197975	19.82
Cal 2-2-1	334441	31.20
Cal 2-2-2	336988	31.20
Cal 2-2-3	335368	31.20

		Sample [cTnl], mg/L	2921a [cTnl], mg/L
2921a-2-1	316247	30.31	153.36
2921a-2-2	304495	29.07	147.08
2921a-2-3	289495	27.49	139.07
2921a-8-1	316778	30.37	151.78
2921a-8-2	308985	29.54	147.67
2921a-8-3	306556	29.29	146.39
2921a-9-1	321326	30.85	153.31
2921a-9-2	317573	30.45	151.34
2921a-9-3	313211	29.99	149.05
2921a-13-1	318297	30.53	152.25
2921a-13-2	318591	30.56	152.40
2921a-13-3	312149	29.88	149.01

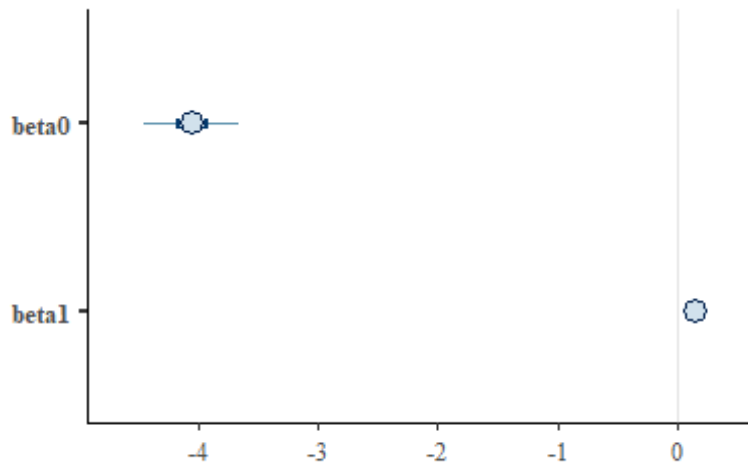
\* = combined SIM peak area from m/z = 825.7, 855.1, 886.8



## Appendix H. Additional statistical results from hierarchical calibration model

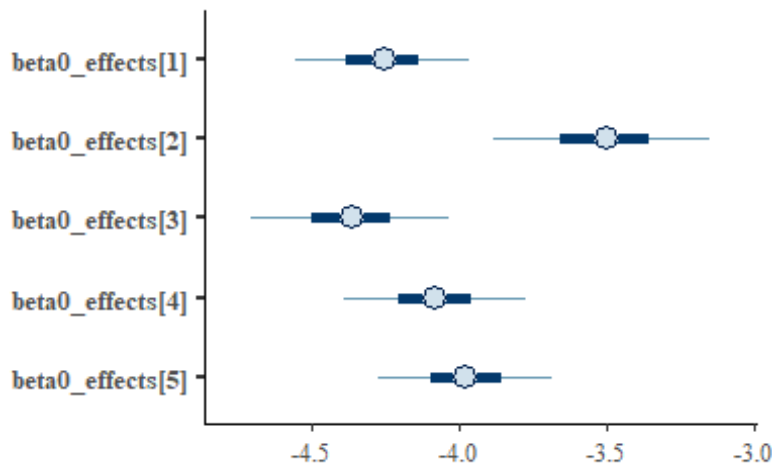
The figures below display posterior distributions from the Calibrant Model. These values aren't immediately relevant to the certified value statement but provide context for the full experimental model.

The first plot summarizes the posterior distributions for the mean slope and intercept of the varying-slope varying-intercept models.



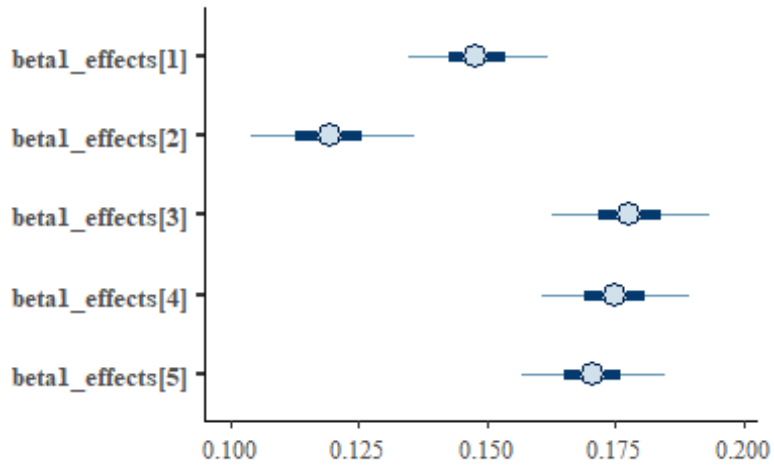
*Posterior for mean slope and intercept.*

The following two plots show the sample-specific estimates and uncertainties for the linear calibration function. Of note is that the slopes and intercepts appear meaningfully different between each sample, as was seen in Figure 1 and was accounted for in the final statistical model.

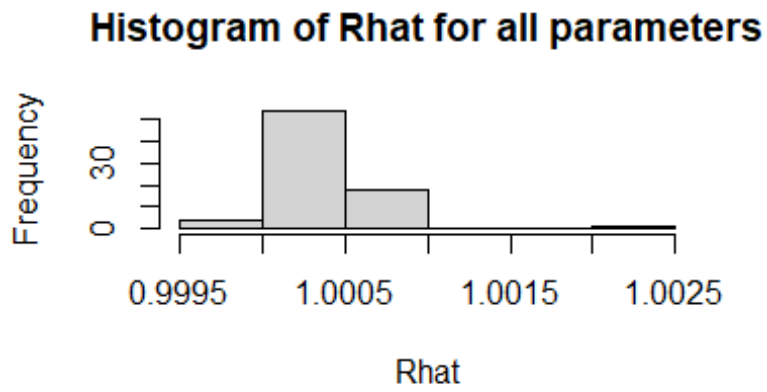


*Posterior for set-specific intercept effects*

Lastly, we provide a histogram of the Rhat diagnostic value for all estimated parameters in the model, indicating that the MCMC chains have likely achieved sufficient convergence during the model fitting process.



*Posterior for set-specific slope effects*



*Histogram of Rhat values across all fitted parameters.*